UNIVERSITY OF CALIFORNIA, SAN DIEGO

The Role of Macrophage Chemoattractant Signaling in Cancer Cell Migration, Metastasis and Neovascularization

A thesis submitted in partial satisfaction of the requirements for the degree Master of Science

in

Biology

by

Tiffany Liu

Committee in charge:

Professor Randall S. Johnson, Chair
Professor Richard L. Klemke, Co-chair
Professor Colin C. Jamora

2010

ProQuest LLC
789 East Eisenhower Parkway
P.O. Box 1346
Ann Arbor, MI 48106-1346

The Thesis of Tiffany Liu is approved, and it is acceptable in quality and form for publication on microfilm and electronically:

_____

_____
Co-Chair

_____
Chair

University of California, San Diego

2010

DEDICATION

This is dedicated to my family for their love and patience, my friends for their honest support and to my teachers who've reaffirmed my curiosity for science. I am a better student and scientist because of you.

TABLE OF CONTENTS

LIST OF ABBREVIATIONS

CAM	(Chicken) Chorioallantoic Membrane
CSF-1	Colony Stimulating Factor-1, also called M-CSF
DsRed	*Discosoma sp.* Red Fluorescent Protein
GFP	Green Fluorescent Protein
HPRT-1	Hypoxanthine Phosphribosyltransferase-1
MAB	Migration Adhesion Buffer
SDF-1α	Stromal Derived Factor-1 alpha
TAM	Tumor Associated Macrophage
VEGF-A	Vascular Endothelial Growth Factor A

LIST OF FIGURES AND TABLES

ACKNOWLEDGEMENTS

I would like to thank my adviser Professor Richard Klemke for his guidance and support during my studies, Chad E. Green, Konstantin Stoletov and Barry Wang for answering my endless questions, and current and former members of the Klemke lab for their help.

I would also like to thank Valerie Montel and Robin D. Lester formerly of the Steven Gonias Lab for their collaborative work in hypoxia and macrophages.

Special thanks also to Shankar Subramaniam and his lab for their collaborative work on profiling gene expression in our macrophage and cancer cells.

The Methods, in full, is a reprint of the material as it appears in Green CE, Liu T, Montel V, Hsiao G, Lester RD, Subramaniam S, Gonias SL Klemke RL. (2009) Chemoattractant Signaling between Tumor Cells and Macrophages Regulates Cancer Cell Migration, Metastasis and Neovascularization, *PLoS One*. 4(8): e6713. The thesis author was a primary investigator and second author of this paper.

The Results, in part, is a reprint of the material as it appears in Green CE, Liu T, Montel V, Hsiao G, Lester RD, Subramaniam S, Gonias SL Klemke RL. (2009) Chemoattractant Signaling between Tumor Cells and Macrophages Regulates Cancer Cell Migration, Metastasis and Neovascularization, *PLoS One*. 4(8): e6713. The thesis author was a primary investigator and second author of this paper.

ABSTRACT OF THE THESIS

The Role of Macrophage Chemoattractant Signaling in Cancer Cell Migration, Metastasis and Neovascularization

by

Tiffany Liu

Master of Science in Biology

University of California, San Diego

Professor Randall S. Johnson, Chair
Professor Richard L. Klemke, Co-chair

Tumor-associated macrophages possess the potential to contribute to cancer progression by modulation of immune function, angiogenesis, and cell metastasis. However, understanding of the chemokine signaling networks that regulate this process is unclear. Here, we demonstrate that treatment of CT26 colon cancer cells with RAW 264.7 macrophage conditioned media induces cancer cell migration, invasion and metastasis. Genetic profiling indicated that chemokines SDF-1α and VEGF are

upregulated in tumor-stimulated macrophages and contribute to tumor cell migration in vitro. Macrophages also showed a robust chemotactic response towards tumor-derived chemokines. Microarray analysis and functional testing revealed CSF-1 as the major chemoattractant for macrophages. In the *in vivo* CAM model, RAW macrophages localized specifically to the tumor periphery where they were found to increase CT26 tumor growth, microvascular density, vascular disruption, and lung metastasis suggesting these cells home to actively invading areas of the tumor, but not the hypoxic core of the tumor mass. Additionally, hypoxic conditions down-regulated CSF-1 production in several tumor cell lines and decreased macrophage migration in vitro. Taken together our findings suggest that normoxic tumor cells release CSF-1 to recruit macrophages to the tumor periphery where they secrete mitogenic and angiogenic factors that facilitate tumor cell proliferation, invasion and metastasis.

1. Introduction

1.1 Inflammation and the Tumor Microenvironment. Tumor malignancy is a dynamic process that results from microenvironment changes working in concert with defined oncogenic mutations. An increased risk of malignancy is associated with some chronic inflammations which result in genetic events that cause neoplastic transformation (e.g. *Helicobacter pylori* for gastric cancer). However, many inflammatory cells and their mediators are often found in the microenvironment of cancers that are unrelated to infectious conditions where they are found to contribute to disease progression. Thus the development of an inflammatory microenvironment promotes the advancement of tumor malignancy.

The tumor stroma is made of many cell types that have the potential to benefit tumor progression such as fibroblasts, adipocytes, endothelia, perivascular and immune cells (1). Macrophages represent a major portion of the tumor immune cell infiltrate, however there is great functional heterogeneity in these highly plastic cells (2). Subpopulations function in tissue remodeling, inflammation and immunity, and have the capacity to affect neoplastic tissues in vascularization, migration and proliferation providing both beneficial and inhibitory effects on tumor growth and progression to late stage disease (3, 4). It is believed that macrophages can be educated by the tumor microenvironment to adopt roles that facilitate the metastatic process. For example, in early stages of tumorigenesis, macrophages have been found at points of basement membrane breakdown and at the invasive edges of advanced tumors. Suggesting tumors exploit the matrix remodeling features of macrophages (5).

1.2 Tumor-Associated Macrophages. Tumor-associated macrophages (TAMs)

are macrophages whose functional lineage have been selectively conditioned to support tumor development. These macrophages are thought to be derived from circulating peripheral blood monocytes that are attracted to the tumor vasculature where they extravasate into the stroma (6). Although the process is poorly understood, tumor cells are known to release macrophage chemoattractants including CCL2, 5, 7, and 8, SDF-1α, VEGF and CSF-1 (7). Classically activated macrophages (M1) function as primary effector cells of the innate immune system, killing micro-organisms and tumor cells and produce proinflammatory cytokines. In contrast, TAMs (M2) promote local angiogenesis, tissue remodeling and repair; supporting tumor survival while suppressing the normal immune response (8). Moreover, TAMs localize to the invasive areas of the tumor where they can secrete a variety of cytokines and proteases that elicit the invasion and metastasis of tumor cells into surrounding tissues (9, 10). In this role, TAMs actively contribute to tumor progression and the transition to malignancy that often correlates with poor clinical outcome.

1.3 Angiogenesis. Angiogenesis and increased microvascular density are critical steps in the progression of cancer malignancy that can be initiated by a variety of factors known to stimulate vessel growth. As a primary sources of angiogenic proteins (VEGF, TGF-β, EGF, bFGF and TNF-α), TAMs are directly involved in the regulation of neovascularization in the tumor microenvironment (2, 11, 12). In particular, VEGF is a potent stimulus for the growth of new vessels, increased microvascular density, vascular disruption and leak (13). Remodeling vessels are porous and fragile and thus more susceptible to tumor cell intravasation (14, 15). Therefore, it is likely TAMs at the invasive front of the tumor may promote tumor metastasis by stimulating the formation

of dense microvascular networks of leaky vessels that are permissible to tumor cell intravasation, while simultaneously activating the migration and invasive machinery of tumor cells through mitogen signaling.

1.4 Hypoxia. Studies regarding hypoxia and inflammation indicate that TAMs may accumulate preferentially in the poorly vascularized region of tumors (16), where they are stimulated to promote angiogenesis and play a role in extracellular matrix remodeling (17, 18). Thus, hypoxia represents a major environmental stress factor that affects the biology of TAMs.

TAMs are thought to be attracted to the hypoxic tumor core in response to VEGF release as well as cell debris and other factors released by avascular, necrotic tumor cells (19, 20, 21). Once localized to the core, TAMs clear cellular debris and regulate vascularization to contribute to tumor survival. Thus, there are likely subsets of these macrophages that are differentially distributed in the tumor microenvironment that play specialized roles during cancer progression (3). For example, the role of TAMs in the hypoxic tumor core may be primarily angiogenic and phagocytic, whereas under normoxic conditions at the tumor periphery TAMs may contribute to tumor metastasis by increasing tissue remodeling and vascular density. In the latter case, VEGF release by TAMs may be regulated independently of hypoxia through interactions with invasive tumor cells or stromal cells.

1.5 Signaling Molecules. Chemotactic cytokines are more than cell attractants in tumors. Transcriptional profiling has shown that chemokines can activate distinct functional progress in monocytes in addition to their roles in the recruitment and positioning of TAMs in tumors and surrounding stroma (22, 23, 24).

CSF-1 has been implicated for its role in metastasis as a regulator of TAM produced tumor cell growth factors, matrix metalloproteinases and angiogenic factors. It is also described as part of a paracrine loop, along with EGF, that enhances the migratory phenotype of tumor cells (25).

In a landmark study, a CSF-1 knockout was made in PyMT mice such that the resulting mammary tumors formed were unable to accumulate macrophages. Though incidence and rates of growth of the primary tumors were unaffected, the rate of tumor progression was slowed with limited metastatic capacity. Exogenous addition of CSF-1 restored the rates of metastasis to wild-type levels. In addition to this, wild-type mice overexpressing CSF-1 showed accelerated rates of tumor progression and increased metastases (26). This study also points to the interesting distinction in the role of CSF-1 mediated TAMs in initial tumor onset versus tumor progression and metastases.

Many other chemokines and their receptors have been rigorously studied for their roles in tumor progression. In a study investigating chemokine receptors in the targeted metastasis of breast cancer cells, researchers strongly correlated the presence of CXCR4 and its ligand SDF-1α in breast cancer cells and target organs. Protein lysates made from organs belonging to the breast cancer metastatic cascade (lymph node, lung, liver) were tested against breast cancer cells, which highly express CXCR4, for chemotactic activity. The increased cancer cell migration induced by these extracts was significantly reduced by blocking antibodies for CXCR4 and SDF-1α. This relation was reproduced in *vivo*, when qPCR revealed that neutralizing the interaction between SDF-1α /CXCR4 significantly impaired metastasis of breast cancer cells (27).

1.6 Aim of Study. The presence of macrophages in primary tumors is associated

with increased metastatic potential and poor prognosis for the majority of reported clinical and genetic studies including breast, prostate, ovarian and cervical cancers. (25, 28) However, the mechanism is unknown and its pathological significance of in others cancers, including colorectal cancer, remains unclear (29). To test the effect of CSF-1, EGF and other possible chemokines in promoting tumor progression and metastases, former postdoc Chad E. Green began a project studying the effects of mouse macrophage RAW264.7 when co-cultured with CT26 colon cancer cells. He showed that co-culture of the two cell types increased the migratory profile of the CT26 cancer cells, which adopted a more mesenchymal phenotype that correlated with increased persistence in migrational behavior. Both showed increased migration towards conditioned media, however the recruitment of CT26 cells by RAW 264.7 is not necessarily dependent on EGF. Elisa-based gene array analysis performed on the cells when exposed to contrasting conditioned buffers showed the up-regulation of many chemokines as possible candidates for chemoattractantion.

Here, I have reproduced his results in an *in vivo* chicken embryo xenograft model, as well as explored other possible candidates that increase the migratory profile of these two cell types in *in vitro* chemotaxis assays. I show that, in agreement with previously published data, macrophages promote tumor progression and infer increased metastatic potential on cancer cells *in vivo*.

2. Materials and Methods

2.1 Cell Lines, Reagents and Antibodies. CT26 mouse colon cancer, RAW 264.7 mouse macrophage and MDA-MB-468 breast cancer cell lines were obtained from American Type Culture Collection (ATCC, Manassas, VA). The CL16 cell line, a metastatic variant of MDA-MB-435, was derived as previously described (30). CT26 cells were maintained in RPMI 1640 supplemented with 10% FBS, 1% penicillin-streptomycin (Invitrogen, Carlsbad CA) and 1% glutamine. RAW 264.7, MDA-MB-468 and CL16 cells were cultured in DMEM (Invitrogen, CA) supplemented with 10% FBS, 1% penicillin-streptomycin and 1% glutamax (Invitrogen, Carlsbad CA). RAW 264.7 expressing GFP were made by infecting cells with Lenti-Green supernatant (BioGenova, Rockville, MD). The highest 0.1% expressing cells were then sorted by FACS. CT26 cells expressing DsRed were generated by infecting cells with the lentivirus, pEF1-DsRed-pur, followed by selection in puromycin (1 μg/ml). Where indicated, cells were treated with blocking anti-CSF-1R mAb (AFS98, eBioscience, San Diego, CA), blocking anti-EGF-R (Millipore, Billerica, MA), recombinant mouse CSF-1 (R&D Systems, Minneapolis, MN), recombinant mouse SDF-1α (Millipore, Billerica, MA) or VEGF165 (Millipore, Billerica, MA).

2.2 Timelapse Imaging of Cell Morphology and Migration Behavior. For timelapse imaging of cell migration in co-culture, RAW 264.7-GFP were incubated on fibronectin (10 μg/ml, Sigma-Aldrich) coated Lab-Tek chamber slides (Nunc, Rochester, NY) for 30 min at 37°C prior to addition of CT26-DsRed (10^7 cells/ml). Once CT26 were added, the chamber slide was immediately placed in an Inc-2000 Incubator System (20/20 Technology Inc., Wilmington, NC) then imaged at 20X (NA = 0.75) for 15 hrs at

4 frames/hr using a Nikon C1-Si inverted confocal microscope (Nikon Instruments Inc., Melville, NY) equipped with PMT detectors and lasers appropriate for GFP (488 nm) and DsRed (561 nm). Descanned images were acquired using Nikon EZ-C1 software then rendered for cell tracking and shape analysis using Imaris (Bitplane, Saint Paul, MN). Upon adhesion, the location coordinates of centroids for individual CT26-DsRed cells were recorded at each frame over the timecourse of migration. These coordinates were then used to create migration tracks from which the migration straightness, displacement and total distance were determined. Migration straightness is a unitless value that relates the number of branch points or turns in a track to the total migration distance. Total migration path length was determined by summing migration step distances every frame throughout the video sequence. Net migration path displacement was quanitated as the direct distance between the start of migration and the end of migration. The shape index is the ratio of the major axis length over the minor axis length for individual cells tracked over the timecourse of migration.

2.3 Chemotaxis and Invasion Assays. Chemotaxis assays were performed as previously described with minor modifications (31). Briefly, modified Boyden chambers (Transwell, 6.5 mm diameter; Corning, Lowell, MA) containing polycarbonate membranes with 8 μm pores were coated on both sides with fibronectin (10 μg/ml, Sigma-Aldrich) for 2 h at 37°C, rinsed once with PBS, and then placed into the lower chamber containing 500 μl migration adhesion buffer (MAB; DMEM with 0.1% RIA-grade fraction V BSA (Sigma-Aldrich), 1% penicillin-streptomycin and 1% glutamine), complete media (DMEM supplemented with 10% FBS, 1% penicillin-streptomycin and 1% glutamine), conditioned media or serum-free migration buffer containing SDF-1α

(100 ng/ml), VEGF165 (10 ng/ml), EGF (100 ng/ml) or CSF-1 (40 ng/ml), as indicated. Conditioned medias were collected from CT26 or RAW 264.7 cultures following 48 hrs of incubation at 37°C. Dilutions of conditioned medias were made in appropriate base culture media. Where indicated, anti-CSF-1R (20 μg/ml) and anti-EGF-R (20 μg/ml) were present in both top and bottom wells throughout the assay. Serum-starved RAW 264.7 or CT26 cells were removed from culture dishes with Hanks' balanced salt solution containing 5mM EDTA and 25 mM Hepes, pH 7.2, and 0.01% trypsin, washed twice with migration buffer, and then resuspended in migration buffer at 10^6 cells/ml. 10^5 cells in 100 μl migration buffer were then added to the top of each migration chamber and allowed to migrate to the underside of the porous membrane for various times in triplicate. RAW 264.7 migrated for 24 hrs in all conditions and CT26 migrated for 3 hrs in all conditions. The nonmigratory cells left on the upper membrane surface were removed with a cotton swab, and the migratory cells attached to the bottom surface of the membrane were stained with 0.1% crystal violet in 0.1 M borate, pH 9.0, and 2% ethanol for 20 min at room temperature. The numbers of chemotaxing cells per membrane were counted using an inverted phase contrast microscope at 40X.

To examine macrophage invasion into collagen, CT26-DsRed or red fluorescent (580 nm excitation/605 nm emission) polystyrene microspheres (10 μm; Molecular Probes, Carlsbad, CA) were embedded in sterile filtered type 1 collagen gel (PureCol; Nutacon, Leimuiden, The Netherlands) containing 1X RPMI (Sigma-Aldrich), 25 mM sodium bicarbonate and adjusted to pH 7.4 using 0.1 M sodium hydroxide, as previous described (32). The collagen solution containing CT26-DsRed (10^7 cells/ml) or beads (10^7 beads/ml) was allowed to gel in 10 μl aliquots on fibronectin (10 μg/ml, Sigma-

Aldrich coasted Lab-Tek chamber slides (Nunc, Rochester, NY) for 20 min prior to addition of RAW 264.7-GFP (10^5 cells/ml). Initial migration of RAW 264.7-GFP at the interface with the collagen drop was imaged at 20X (NA = 0.75) for 12 hrs at 4 frames/hr using a Nikon C1-Si inverted confocal microscope (Nikon Instruments, Inc., Melville, NY) equipped with PMT detectors and lasers appropriate for GFP (488 nm) and DsRed (561 nm). Descanned images were acquired using Nikon EZ-C1 software then rendered for cell tracking using Imaris (Bitplane, Saint Paul, MN). Location coordinates of centroids for individual RAW 264.7-GFP were recorded at each frame over the timecourse of migration. These coordinates were then used to calculate the displacement and total distance migrated for cells within and beyond 100 μm of the collagen drop boundary. Slides were incubated for an additional 7 days then imaged using confocal microscopy (20X; NA = 0.75) at 1 μm increments throughout the entire Z-axis of the collagen drop.

2.4 Microarray Analysis. To examine inflammatory gene expression, conditioned medias were collected from CT26 or RAW 264.7 cultures following 48 hrs of incubation at 37°C and applied to starved cultures of the opposing cell type for 24 hrs. mRNA was then isolated using the RNeasy kit (Quiagen, Valencia CA), reverse transcribed using the iScript cDNA synthesis kit (Bio-Rad Laboratories, Hercules, CA) and analyzed by hybridization to the Codelink Mammalian Inflammatory Bioarray (GE Healthcare, Piscataway, NJ), according to the manufacturer recommendations. Significance of transcript upregulation or downregulation was determined using the VAMPIRE statistical algorithm, as previously described (33).

2.5 Chicken CAM Assay. The chick embryo metastasis assay was performed as previously described (34, 35). CT26-DsRed alone or combined with RAW 264.7-GFP ($2x10^6$ cells total) cells were suspended in Matrigel (BD Bioscience) on ice then inoculated onto the chorioallantoic membrane (CAM) of a 9 day old chick embryo. On developmental day 20, embryos were sacrificed and primary tumors were removed, imaged at 0.63X and 2X by stereomicroscopy, weighed and measured for diameter. Once heart and lungs were isolated, cell dissemination was quantified by counting cell clusters at 20X by stereomicroscopy. Tumors were subsequently sectioned and placed directly onto a glass coverslip for imaging by confocal microscopy at 20X. Tumors were imaged at 0 cm from the periphery or edge (tumor periphery), 0.5 cm from the periphery (tumor wall) and 1.0 cm from the tumor periphery (tumor core). Quantitation of RAW 264.7-GFP distribution within the CT26-DsRed tumors was determined by averaging GFP pixel bit maps over a field of view to produce a mean fluorescence intensity for each region of the tumor using Image Pro Plus v. 4.5 (Media Cybernetics, Bethesda, MD). Brightness and contrast adjustments were made equally to all channels and did not modify the relative differences between GFP pixel intensity in various regions of the tumor.

2.6 qPCR. CT26, MDA-MB-468 or CL16 tumor cells were incubated at 37°C in the appropriate complete medium for 24 hrs under hypoxic (1.0% oxygen) or normoxic (21% oxygen) conditions. Total RNA was then extracted using TRIzol (Invitrogen, Carlsbad CA), according to the manufacturer recommendations. cDNA was synthesized from 2 μg of total RNA using the iScript cDNA synthesis kit (Bio-Rad Laboratories, Foster City, CA) and a one-step program: 95°C, 10 min; 95°C, 30 sec; 60°C, 1 min for 40

cycles. CSF-1 and GAPDH mRNA levels were measured in triplicates and normalized against HPRT-1 mRNA.

2.7 Hypoxic/Normoxic Chemotaxis Assays. For RAW 264.7 chemotaxis under hypoxic conditions, the lower chambers were supplemented with complete DMEM containing 10% FBS to create a chemotactic gradient. RAW 264.7 were then allowed to migrate for 24 hrs under normoxic (21% oxygen) or hypoxic (1% oxygen) conditions using an IsoTemp incubator (Fisher Scientific, Pittsburgh, PA. Migratory cells were fixed with 10% methanol for 5 min and stained with 0.1% crystal violet in 0.1 M borate, pH 9.0, 2% ethanol for 20 min. Membranes were cut from the Transwell and placed in 200 μl of 10% acetic acid to elute the stain then absorbance was read at 570 nm.

2.8 Statistical Analysis. Data analysis was performed using GraphPad Prism version 4.0 software (GraphPad Software, San Diego, CA). All data are reported as mean ± SE. Nonparametric group data were analyzed by analysis of variance (ANOVA) and the Neuman-Keuls post-test. Gaussian-distributed mean values were analyzed by Student *t* test. Group comparisons were deemed significant for 2-tailed *P* values below 0.05.

2.9 Acknowledgment. The Methods, in full, is a reprint of the material as it appears in Green CE, Liu T, Montel V, Hsiao G, Lester RD, Subramaniam S, Gonias SL Klemke RL. (2009) Chemoattractant Signaling between Tumor Cells and Macrophages Regulates Cancer Cell Migration, Metastasis and Neovascularization, *PLoS One*. 4(8): e6713. The thesis author was a primary investigator and second author of this paper.

3. Results

3.1 Migration and Morphological Analysis of CT26 Cancer Cells Co-Cultured with RAW 264.7 Macrophages.

To directly examine how macrophages alter the migratory behavior and persistence of colon cancer cells, a kinematic analysis of tumor cell migration behavior was first performed to determine cell shape changes in response to macrophage co-culture. CT26 mouse colon cancer cells were imaged during co-culture for 15 hours in the presence or absence of RAW 264.7 mouse macrophages (Fig. 1A). CT26 cells alone exhibited an overall migration length statistically similar to that of CT26 co-cultured with RAW cells (199 ± 78 mm (SE) vs. 154 ± 46 mm, respectively) (Fig. 1B). Despite this, CT26 in co-culture (straightness value 0.34) migrated along significantly straighter paths than CT26 alone (straightness value 0.15) (Fig. 1B). Co-cultured CT26 cells were significantly increased in persistence than CT26 cells alone (49 ± 24 mm vs. 28 ± 20 mm, respectively) (Fig. 1B). The effect of RAW in co-culture seems limited to enhancing tumor cell migration directionality; overall migration distance did not change. Additionally, RAW macrophages did not constrain CT26 cell viability; rather CT26 cells grew faster in the presence of the macrophages (data not shown). Together these findings indicated that RAW macrophages promote tumor cell proliferation and enhance persistence and directional cell migration on 2D surfaces.

The ability of cancer cells to form invadapodia and membrane protrusions has been linked to increased migration and tissue invasiveness (35). Therefore, we examined CT26 cells for cell shape changes in response to co-culture with RAW macrophages. Within 6 hrs, the RAW macrophages induced a highly mesenchymal cell shape

characterized by numerous long member protrusions that radiated outward from the cell body (Fig. 2A). This morphology was sustained for greater than 12 hrs and was evident in all CT26 cells within the co-culture that were in contact with one or more macrophages (Fig. 2B). To determine the minimum time required for RAW cells to elicit CT26 shape changes, we measured the kinetics of shape change (Fig. 2C). Beginning with initial adhesion of cells to the dish, the major and minor axes of migrating CT26 was determined every 20 min through 12 hours of co-culture with or without RAW cells. As expected, CT26 cells alone or in co-culture were effectively round upon initial adhesion to the dish with shape indices of ~1. Interestingly, CT26 incubated with RAW cells underwent rapid cell elongation, as the major axis along the polarized membrane extensions were ~4-fold longer than the minor axis as early as 4 hrs following initial cell adhesion (Fig. 2C) when compared to cells without RAW. The shape change reached a plateau at ~5.5 after 8 hrs of co-culture. As expected, CT26 alone also exhibited an initial increase in shape extension as they adhere and spread however; these cells only extend short protrusions and fail to elongate significantly reaching a maximum shape index of ~2 after 6 hrs of culture (Fig. 2C). Taken together, quantitative analysis of CT26 migration and morphology dynamics indicate that RAW macrophages elicit a rapid and sustained increase in cell migration that is associated with increased formation of membrane protrusions.

3.2 RAW 264.7 Macrophages and CT26 Tumor Cells Release Soluble Chemotactic Factors that Promote Co-Chemotaxis. We next examined whether the induction of CT26 invasiveness was due to a direct interaction with macrophages or to soluble chemotactic factors released by macrophages using a standard Boyden chamber

assay (31). CT26 cells demonstrated a dose dependent and robust chemotaxis response toward a gradient of RAW conditioned media (CM), whereas exposure to control basal media alone did not induce a migratory response (Fig. 3A). Importantly, cell migration was predominantly directional toward the concentration gradient as tumor cell migration was strongly reduced by (~60%) when RAW CM was added uniformly to both top and bottom chambers (Fig. 3A). These findings indicate that RAW macrophages release soluble factors that promote directional migration of CT26 colon cancer cells.

RAW macrophages also exhibited a robust and dose dependent chemotaxis to a gradient of CT26 CM (Fig. 3*B*). Indeed, the extent of cell migration to undiluted CM was ~10-fold greater than basal levels of migration observed in response to either serum containing media or migration buffer containing only bovine albumin. RAW cell migration was highly directional. Again, adding CT26 CM to both upper and lower chambers completely diminished the migration response demonstrating that the observed cell migration was not a result of random chemokinetic movement (Fig. 3B).

We next used a 3D migration assay to further investigate the macrophage chemotactic migratory response towards tumor cells in an environment that more closely models the tumor microenvironment. RAW cell migration behavior along CT26 or rhodamine-labeled latex bead embedded in artificial collagen gel tumors was tracked by confocal microscopy during the initial 12 hrs and after 7 days of incubation. RAW macrophages actively invaded tumor cell but not bead embedded collagen gels. Quantitation of the number of macrophages within a field of view indicated an ~8-fold increase in macrophage invasion when tumor cells were present (data not shown). This demonstrates that CT26-derived soluble attractants are required for RAW cell chemotaxis and that

adhesive interactions with the matrix alone are not haptotactic for macrophages in this model. Interestingly, RAW macrophages at the tumor periphery showed changes in migration behavior within 12 hrs of introduction to CT26 embedded collagen gels (Fig. 3D, E). Moreover, the total displacement of this subpopulation was reduced by ~50% , further supporting a decrease in random movement. Most importantly, track analysis indicated that RAW cells within ~100 mm (yellow tracks) rarely migrated away from the tumor. In contrast, RAW cells beyond ~100 mm (white tracks) of the tumor border exhibited rapid chemokinetic movement with no persistent, directional path (Fig. 3D, E). Our results indicate that CT26 cells secrete potent chemotactic factors that attract macrophages. These findings are interesting in light of the fact that we did not detect changes in the migration behavior of RAW cells when co-cultured directly with CT26 cells. Under these conditions it is likely that the CT26 derived factors may not provide a suitable and stable gradient to direct RAW cell migration. The collective findings indicate that both macrophages and tumor cells release soluble chemoattractants that promote directional cell migration.

3.3 Changes in Gene Expression Profiles Induced by Co-Culturing RAW 264.7 Macrophages and CT26 Colon Cancer Cells. While recent evidence indicates that TAMs promote tumor growth, metastasis and suppress the normal anti-tumor immune response, our understanding of how this complex process is regulated is poorly understood (3, 23). The CT26/RAW in vitro cell system described here supports a model in which tumor cells and macrophages rapidly adopt a chemotactic phenotype due to soluble cytokines released by the opposing cell type. To identify the chemokinetic mediators that regulate this process, we examined the expression of over 900 chemokine

and inflammatory pathway genes following culture of CT26 and RAW cells in buffer conditioned by the opposing cell type. Significance of differential expression was determined using VAMPIRE (Variance-Modeled Posterior Inference of Microarray Data), a Bayesian statistical method that models the dependence of measurement variance on the amplitude of gene expression (33). Rather than the *a priori* fold-change cutoff as a means of examining significance or up- or downregulated gene expression, VAMPIRE accounts for the relationship between signal variance and gene expression to determine a more statistically accurate model of differential gene expression. RAW macrophages in CT26 CB upregulated 251 genes and downregulated 28 genes with fold-change cutoffs of 1.2 and 0.27, respectively (Supplementary Figure I). Similarly, CT26 tumor cells in RAW CB upregulated 71 genes and downregulated 16 genes with fold-change cutoffs of 1.4 and 0.005, respectively (Supplementary Figure II). Hierarchical clustering and annotation of differentially expressed transcripts indicated gene signatures associated with a variety of ontology groups, including cell proliferation, chemotaxis, and angiogenesis for both CT26 and RAW 264.7 in conditioned buffers. A partial list of the mostly highly up- or down- regulated genes from these groups, as well as genes relevant to this model, is presented in Table 1. For example, RAW cells stimulated with tumor cell CB upregulated several angiogenic factors (VEGF-A and TGF-α) and chemoattractants (SDF-1α and CXCL2). Notably, CD14, TGF-α, CCR1, IL-18 and SDF-1α have previously been associated with the phenotypic profile of TAMs (37, 38). Genes downregulated include uPA, lymphotoxin B, CCL4, MMP-2 and TNF-α. Among these, TNF-α is reported to be poorly expressed in TAMs and can be pro-apoptotic to tumor

cells (37). Taken together, CT26 CB stimulates RAW macrophages to produce proliferative, angiogenic and motility factors which could impact cancer progression.

CT26 cells also exhibited relevant changes in their chemokine profile when incubated in RAW CB (Table 1). These genes include VCAM-1, VEGF-A, TGF-α, and CXCL1, all of which are reported to be indicative of a metastatic phenotype (39-42). In addition, GM-CSF, the matrix metalloproteinase MMP-10, and chemokines CXCL10, CCL2, CCL20 AND CXCL2 were also upregulated (Table I). Most importantly, CT26 cells upregulated CSF-1 ~2.6-fold in response to RAW CB. CSF-1 has been shown to be a major chemoattractant for macrophages and it has been linked to TAM regulation and cancer progression in animals (26, 43). Taken together, the chemokine expression profile for both RAW and CT26 cells reflect transcriptional signatures predictive of immune modulation and increased tumor cell and macrophage migration, as well as angiogenesis.

3.4 SDF-1α, VEGF and CSF-1 are Key Regulators of Tumor Cell and Macrophage Chemotaxis. We next sought to determine the primary macrophage-derived chemokines responsible for inducing tumor cell migration. Previous reports identify EGF as a primary cancer cell chemoattractant in breast and other cancers (25) however, EGF failed to elicit a CT26 migrational response in our study (Fig. 4A). Moreover, function blocking anti-EGF-R antibodies failed to block CT26 cell migration in response to RAW CB (Fig.4A). Thus, CT26 migration in response to RAW CB is due to soluble factor(s) other than EGF. Similarly previous reports have linked SDF-1α and VEGF to cancer malignancy and both factors were significantly up-regulated in RAW 264.7 cells exposed to CT26 CB (44, 45). Neither SDF-1α nor VEGF induced CT26 cell migration when added separately to the migration chamber. However, when cells were

stimulated with SDF-1α and VEGF simultaneously, tumor cell migration was increased ~2-fold compared to SDF-1α or VEGF alone (Fig. 4B). Despite this, chemotaxis to SDF-1α and VEGF in combination was ~35% less than chemotaxis to RAW 264.7 conditioned media, suggesting the other unidentified RAW 264.7-derived factors likely contribute to CT26 chemoattraction. Nonetheless, these findings indicate that SDF-1α and VEGF work synergistically to potentiate the chemotaxis of CT26 colon cancer cells.

CSF-1 has been implicated as the exclusive chemoattractant secreted by breast cancer cells for TAMs (25, 26, 43). Gene profiling of CT26 cells indicates upregulation of CSF-1 in the present of RAW CB (Table 1). Therefore, we investigated whether CSF-1 was the soluble cue driving RAW chemotaxis to CT26 tumor cells. The stimulation of cells with purified CSF-1 alone was as potent as 100% CM in eliciting RAW chemotaxis (Fig. 4C). This response was inhibited with function blocking antibodies to the CSF1 receptor (CSF-1R). Likewise, the anti-CSF-1R antibodies reduced RAW cell migration to CT26 CM by ~85%. It is important to note that the CSF-1 present in the CT26 CM represents basal secretion, as the conditioned media was generated by CT26 cells that had not been exposed to RAW cells *a priori*. Once CT26 cells are exposed to RAW CM, transcript analysis indicates that the cells upregulate CSF-1 ~2.6-fold above basal secretion levels (Table 1). Taken together, the data indicates that chemotaxis of RAW macrophages to quiescent CT26 cells is robust and occurs primarily in response to tumor secreted CSF-1, which can be further enhanced by exposure to macrophage derived products.

3.5 RAW 264.7 Macrophages Promote CT26 Tumor Formation, Metastasis,

Vascular Density and Vascular Disruption In Vivo. Our data indicates that the chemokine networks established between RAW 264.7 macrophages and CT26 tumor cells propagate the induction of cell migration and the release of angiogenic factors by both cell types. The acquisition of these features by a developing tumor is essential to the late stage progression of the disease. Therefore, we wanted to determine if the RAW 264.7 induced CT26 migrational changes could potentiate CT26 cancer progression *in vivo*. For these studies, we utilized the common chicken egg chorioallantoic membrane (CAM) assay which allows for the rapid evaluation of tumor formation, angiogenesis and cell metastasis (34, 46). CT26 cells in the presence or absence of RAW 264.7 macrophages were inoculated into chick embryos. After 11 days *in vivo*, the tumors were excised and imaged to assess tumor size and vascularization. Tumor cell dissemination into chick lungs was quantified as a measure for metastasis. CT26 tumors that developed in the presence of RAW 264.7 macrophages exhibited a significant increase in tumor size, vascular density, vascular disruption and leak compare to control CT26 tumors without RAW cells (Fig. 5A, B). Moreover, pulmonary CT26 metastasis was increased ~2-fold when RAW macrophages were present in the tumor (Fig. 5 A, B). CT26 cells were not observed in the chick heart under any condition (results not shown). The dramatic increase in small microvessels and the highly disorganized and disrupted nature of the vessels made quantification of typical vascular perimeters (branch points, and length) impossible (Fig. 5A). This vascular phenotype was observed in greater than 80% of the mixed cell tumors but less than 10% of control tumors. Additionally, a ~2.5-fold increase in pulmonary metastasis accompanied the vascular disruption and increased tumor mass observed in mixed cell tumors (Fig. 5B). This highly malignant phenotype

observed in tumors containing RAW macrophages is consistent with the previous *in vitro* data, suggesting RAW macrophages increase the migratory and metastatic properties of CT26 cancer cells in a manner that is associated with increased vascular density and disruption.

3.6 Analysis of Macrophage Localization in CT26 Tumors In Vivo. Published data suggests macrophages are recruited to sites of solid tumor formation *in vivo* in response to soluble cues (25, 26). However, data regarding macrophage localization with the tumor proper and surrounding microenvironment remains inconclusive. To examine the distribution of RAW 264.7 macrophages in the CT26 tumor in the CAM model, macrophages and CT26 cells were transfected with GFP and DsRed, respectively, and co-transplanted onto chick CAMs. Following 11 days of incubation, the tumors were surgically removed, weighed, measured, and bisected before being placed directly onto an imaging chamber. Confocal images were collected sequentially from the tumor border to central core of the tumor at 10X. Quantification of macrophage distribution was determined by calculating average GFP pixel intensity present in each of the tumor regions. Interestingly, GFP labeled RAW macrophages localized primarily within the first 0.5 cm of the tumor edge, with most concentrated at the tumor periphery (Fig. 6A, B). Moreover, no macrophages were observed at the tumor core (1 cm). This pattern of distribution suggests specific migration of macrophages towards CT26 cells residing at or near the tumor border rather than cells at tumor core.

3.7 Tumor Cell Hypoxia Regulates Expression of CSF-1. While the role of hypoxia in regulation of CSF-1 expression has not been previously determined, we hypothesized that CSF-1 levels may be high at the tumor margin where invading cells are

exposed to an oxygen-rich environment compared to the hypoxic tumor core. To investigate this hypothesis, CSF-1 mRNA levels were quantified in CT26 cells cultured for 24 hours under normoxic and hypoxic conditions. Hypoxia caused a significant reduction in CSF-1 mRNA compared to normoxic cells in CT26 as well as in MDA-MB-468 breast adenocarcinoma and metastatic MDA-MB-435 (CL16) breast adenocarcinoma cells (Fig. 6C), suggesting this response may be widespread in various cancers. As anticipated, hypoxic conditions did not change the level of GAPDH or HPRT-1 in the tumor cells, which served as internal controls (results not shown). Based on these results, we hypothesize that the selective localization of RAW 264.7 macrophages to the tumor periphery occurs in response to a CSF-1 gradient generated between hypoxic and the normoxic regions of the tumor. In support of this, RAW 264.7 macrophages do not migrate effectively under hypoxic conditions characteristic of the tumor core microenvironment (Fig. 6D). Together, the data suggests macrophages home to the tumor periphery during the early stages of tumor growth in response to CSF-1 released by normoxic tumor cells, where they stimulate cell migration, angiogenesis and metastasis.

3.8 Acknowledgement. The Results, in part, is a reprint of the material as it appears in Green CE, Liu T, Montel V, Hsiao G, Lester RD, Subramaniam S, Gonias SL Klemke RL. (2009) Chemoattractant Signaling between Tumor Cells and Macrophages Regulates Cancer Cell Migration, Metastasis and Neovascularization, *PLoS One*. 4(8): e6713. The thesis author was a primary investigator and second author of this paper.

4. Discussion

4.1 Summary. The purpose of this study was to elucidate the chemokinetic signaling mechanisms responsible for the enhanced invasive phenotype adopted by cancer cells in the presence macrophages. Through microarray analysis, we found that in response to CT26 tumor cell conditioned media, RAW 264.7 macrophages adopt an alternative phenotype characterized by upregulation of numerous chemotactic cytokines and angiogenic growth factors, including TGF-β, VEGF, CXCL2 and SDF-1α. Additionally, in response to RAW 264.7 macrophage conditioned media, tumor cells also upregulate numerous chemotactic cytokines and angiogenic factors, including CCL2, CSF-1, CSF-2 and VEGF. Chemotaxis assays confirmed that RAW 264.7 macrophages are highly chemotactic to tumor derived CSF-1, whereas CT26 tumor cells in this system chemotax to a combination of VEGF and SDF-1α but not EGF, as has been previously described in other cancers (25). *In vivo* RAW 264.7 macrophages localize to the tumor periphery where they potentiate CT26 tumor cell metastasis and neovascularization in the CAM model. Finally, qPCR showed CT26 tumor cells exposed to hypoxia downregulate CSF-1 expression, suggesting a preliminary mechanism for macrophage homing to the tumor periphery rather than the tumor core.

The data presented here indicates that RAW 264.7 macrophages affect CT26 tumor metastasis (and subsequent disease progression) by two means. First, close contact co-culture results in an enhanced mesenchymal phenotype in CT26 cancer cells. The resulting changes in migrational behavior produce a more persistently migrating

population of tumor cells. Secondly, macrophages produce numerous chemokines and angiogenic factors involved in signaling networks that induce neovascularization and metastasis.

4.2 Chemokines of Interest. Individually, many chemokines have been identified and studied for their effects on tumor metastasis, angiogenesis, proliferation and overall disease progression. However global signaling networks involved in macrophage-tumor cell response have yet to be established, as efforts are likely complicated by multifold redundancy in chemokine function. Additionally, the presence of immune cell subpopulations, immunogenic and immunoevasive, further complicate efforts to clarify these networks.

Previous reports of a paracrine signaling loop between breast cancer cells and macrophages wherein CSF-1 released by breast cancer cells attract macrophages which in turn respond with EGF (25, 43). In our study however, EGF had little effect on CT26 colon cancer cell migration. Although many of the chemokines released by RAW 264.7 cells may contribute to tumor cell migration, we chose to investigate SDF-1α and VEGF as previous reports have linked these factors to cancer malignancy and both factors were significantly up-regulated in RAW 264.7 cells exposed to CT26 CB (44, 45). Synchronous stimulation of VEGF with SDF-1α accounted for the majority of CT26 cancer cell migration towards macrophages, though other unidentified RAW 264.7-derived factors likely contribute to CT26 chemoattraction. This suggests that co-signaling from CXCR4 (SDF-1α receptor) and the tyrosine kinase VEGF receptor(s) are necessary to drive cell migration in this system.

We believe that in close proximity, CT26 cancer cells induce multiple signaling loops in RAW 264.7, using SDF-1α and VEGF-A as chief signaling molecules. Previous work has demonstrated an important role for SDF-1α in mediating colon cancer cell migration and metastasis and VEGF has also been previous linked to cell migration (44, 47). SDF-1α upregulates the expression of VEGF (47) and VEGF in turn upregulates CXCR4 (48). CXCR4 has been reported to be expressed on many leukycotes, including immature and mature monocytes, as well as endothelial cells (50). Macrophages recruited to the tumor may stimulate cancer cells to further increase CSF-1 production. The local development of high CSF-1 concentrations could play a role in maintaining significant levels of resident macrophages in the tumor microenvironment. The resident macrophages, in turn, may be induced to secrete VEGF and SDF-1α to facilitate cell invasion, angiogenesis, and tumor cell dissemination by signaling local stromal and tumor cells.

4.3 Hypoxia and TAM Localization. Existing work indicates that macrophages target the outer perimeter of the tumor where they contribute to cancer invasion and angiogenesis. However, in other cases macrophages can localize within the tumor interior where they are believed to facilitate the removal of dead cells and debris (19). The macrophages imaged in our in vivo CAM experiments were not found in the hypoxic core of tumors but rather the rapidly growing invasive front. Both CSF-1 and hypoxic conditions within the tumor might be responsible for signaling the invasion of macrophage precursors into the tumor (51). Our data also shows that CSF-1 is downregulated in hypoxic conditions, further supporting the model of multiple macrophage subpopulations which localize in different areas of the tumor for their

various functions. We hypothesize that high oxygen tension at the tumor periphery and low oxygen tension at the tumor core create a chemoattractant gradient of CSF-1. The subpopulation observed in our study likely migrates along this CSF-1 gradient towards the actively invading CT26 cells, where they contribute to metastasis rather than tumor homeostasis. While preliminary, this mechanism could direct macrophages to the tumor edge where they further amplify CSF-1 concentrations through positive feedback mechanisms as discussed above. In addition, RAW 264.7 macrophages show reduced ability to migrate under hypoxic conditions, which further supports macrophage localization to the tumor edge and not the hypoxic tumor core.

4.4 Angiogenesis. Vascular remodeling and increased metastasis are important consequences of this process. We observed that the RAW 264.7 macrophages induced a dramatic increase in microvascular density surrounding the CT26 tumor. In fact, the vessels were so disrupted and leaky that it precluded direct enumeration of vessel changes. Although the angiogenic mechanisms that generate this type of response have not been fully elucidated, previous studies have shown that both tumor cells and TAMs express VEGF (44, 52). This suggests that the paracrine signaling between tumor cells and TAMs may be sufficient to induce the release of angiogenic factors in the absence of hypoxia. The resulting high concentration of VEGF would be expected to drive vascular remodeling and permeability which in turn provides an environment rich for tumor growth and metastasis. In fact, disrupted neovasculature has been shown to provide portholes for invasive cancer cells to access the vascular compartment (15). This combined with the known ability of TAMs to secrete extracellular matrix proteases leading to increased tumor cell invasion could account for the increased cell metastasis

associated with TAM infiltration (53). Ultimately, the destabilized vasculature combined with increased tumor cell invasion provides an environment rich for cancer metastasis.

4.5 Future Research and Therapeutics. In an interesting study, known markers for inducible macrophage populations were used to identify and monitor invasive and non-invasive macrophage subpopulations in colorectal carcinomas. 27E10 acute inflammatory macrophages were localized to invasive edge of the tumors where they promoted tumor cell migration but inhibited proliferation. Resident (25F9) and anti-inflammatory (RM3/1) macrophages were found in the tumor center and non-invasive areas of the tumor where they aided tumor cell proliferation but inhibited migration (54). This study shows that the use of proper markers for inflammatory and anti-inflammatory subpopulations is important for the selective targeting of invasive subpopulations. At present, the use of macrophage infiltration as a prognostic indicator is unreliable, especially when considering the great heterogeneity of microenvironments for different tumor types. However, it points to the importance of proper identifying this population of cells within the tumor. Additionally, future research might concentrate on ways to downregulate the TAM functions that are advantageous to tumors and upregulate those that induce an immunological resistance to the tumor cells. Macrophage infiltration involves monocyte recruitment and localization, M2 differentiation, TAM signaling for angiogenic and proliferative events, TAM localization and multiple paracrine interactions with cancer cells, endothelial cells, etc. (38). Each part of this process represents new targets for new pharmaceutical therapies.

4.6 Conclusion. Here, we've presented a model of TAM interaction with colorectal carcinoma cells *in vitro* and *in vivo*. Treatment of CT26 cells with RAW 264.7

conditioned medium induces cell migration, invasion and metastasis. Inflammatory gene microarray analysis indicated CT26-stimulated RAW 264.7 macrophages upregulate SDF-1α and VEGF, and that these cytokines contribute to CT26 migration in vitro. CSF-1 was identified as the major chemoattractant for RAW 264.7 macrophages. *In vivo*, RAW 264.7 macrophages localized specifically to the tumor periphery where they were found to increase CT26 tumor growth, microvascular density, vascular disruption, and lung metastasis, suggesting these cells home to actively invading areas of the tumor, but not the hypoxic core of the tumor mass. It is our hope that the data presented here provides some leverage in the ambitious challenge of delineating tumor cell and microenvironmental signal mechanisms that governs disease progression.

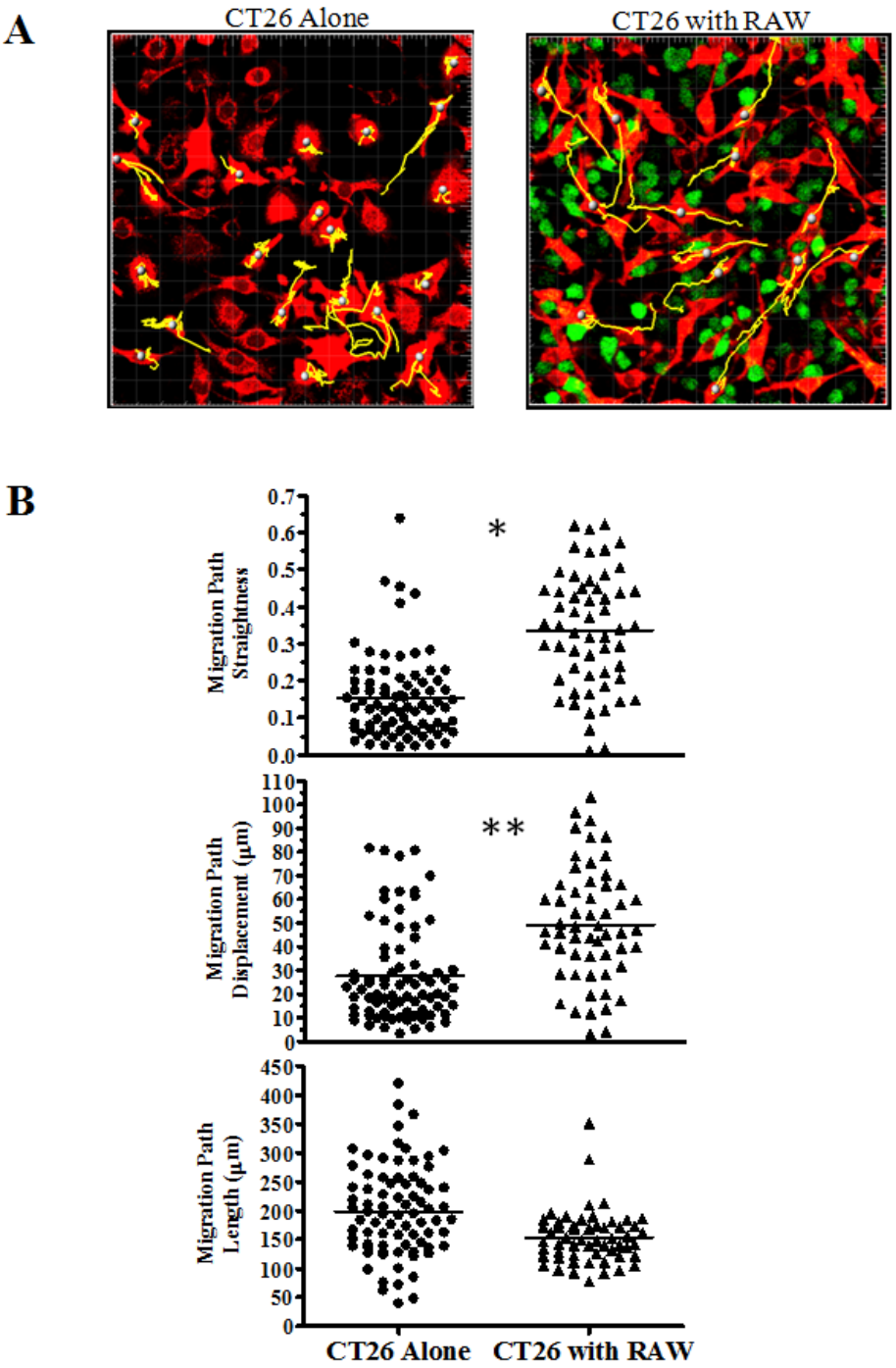

Figure 1. Macrophages elicit directed migration of colon cancer cells *in vitro*. (A,B) CT26-DsRed were incubated with RAW-GFP on fibronectin coated coverslips, as indicated, for 12 hrs at 37°C. During this time, the straightness, total length traveled and total cumulative displacement of individual CT26 cell centroids were tracked (yellow lines) at 4 frames/hr by confocal microscopy (20X). Data is presented as individual track quantitation for 55-75 cells over 3 experiments, with average indicated by bar. * denotes significant difference in migration path straightness ($p < 0.0001$). ** denotes significant difference in migration path displacement ($p < 0.0001$).

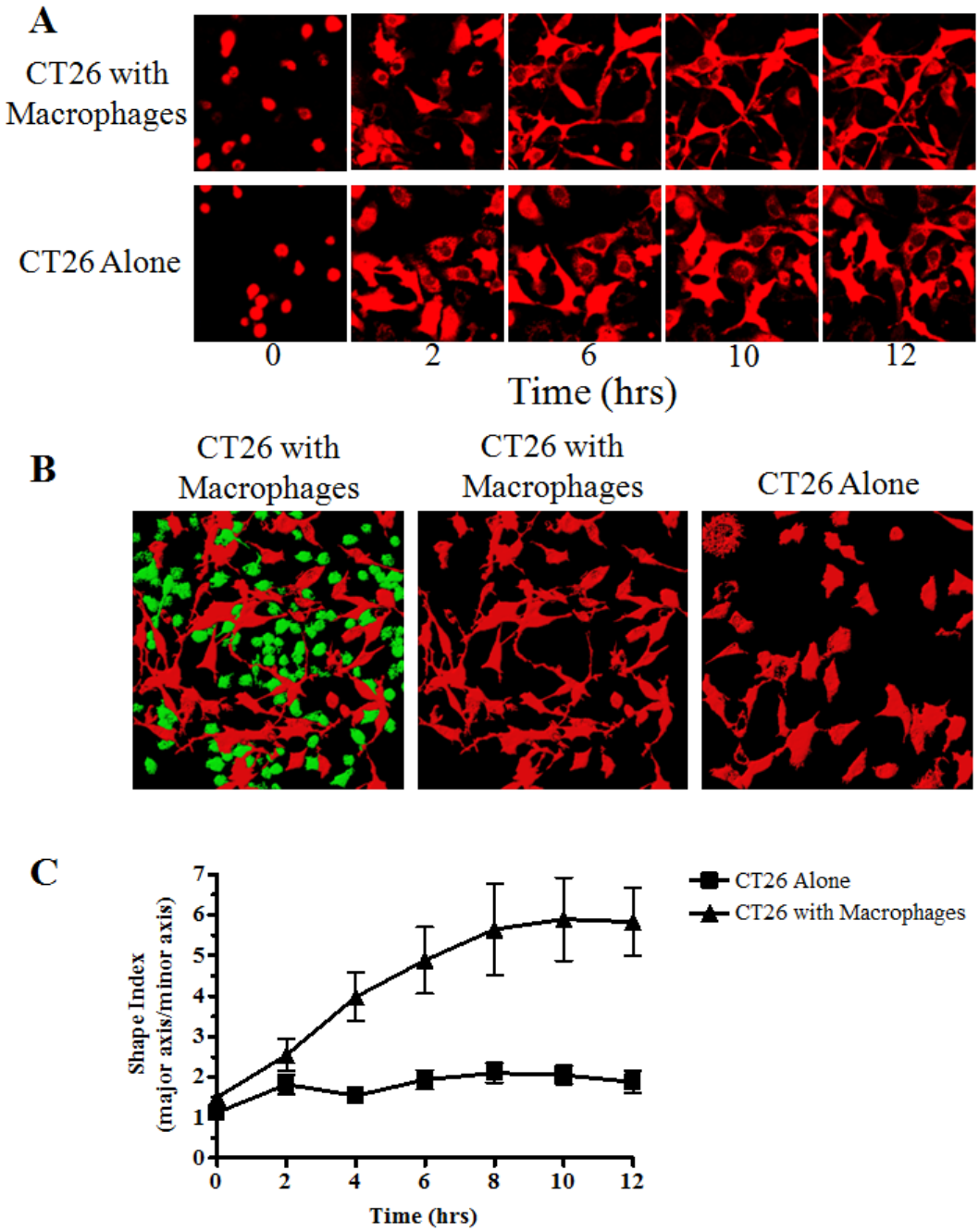

Figure 2. Colon cancer cells exhibit elongated protrusions when cultured with macrophages *in vitro*. Fluorescent images were acquired using confocal microscopy (20X) at 4 frames/hr. A) Time course of CT26-DsRed dynamics over 12 hrs when incubated alone or with GFP-RAW 264.7 macrophages. Images are representative of CT26 movement over 3 separate experiments. (B) Cumulative CT26-DsRed distribution and protrusion after 15 hrs of incubation alone (right) or with GFP-RAW 264.7 macrophages (left and center, with green channel turned off). Images are representative of 3 separate experiments. (C) The shape index (major axis/minor axis) of CT26 cells in the presence or absence of RAW 264.7 cells was tracked over 12 hrs of migration (mean ± SEM; n = 10 cells over 3 separate experiments).

Figure 3. Macrophages and colon cancer cells chemotax to soluble cues. (A) CT26 were added to the upper of a Boyden chamber with RAW 264.7 conditioned media, control buffer or complete DMEM added to the lower well. Studies were performed for 3 hrs at 37°C (mean ± SEM; *n* = 15-30 randomly selected fields over 3-6 separate experiments). * denotes significance between 50% RAW CM and media control ($p < 0.001$) and 50% RAW CM and 100% RAW CM top/bottom ($p < 0.001$). (B) RAW 264.7 were added to the upper well of a Boyden chamber with CT26 conditioned media, control buffer or complete DMEM added to the lower well. Studies were performed for 24 hrs at 37°C (mean ± SEM; *n* = 15-30 randomly selected fields over 3-6 separate experiments). ** denotes significance between 25% CT26 CM and media control ($p < 0.001$) and 25% CT26 CM and 100% CT26 CM top/bottom ($p < 0.001$). (C) RAW-GFP macrophage invasion was imaged after 7 days by confocal microscopy (20X). Side view and top view images are representative of the average macrophage response over 6 collagen tumors. (D) The interface between macrophages and the collagen tumor drop was imaged using confocal microscopy (20X) for 12 hrs at 4 frames/hr following addition of RAW 264.7 to the chamber slide. Macrophage migration was quantitated by tracking individual cell centroids at 4 frames/hr. Macrophages initiating migration within 100 μm of the tumor boundary (dashed white line) exhibit yellow tracks. Macrophages initiating migration beyond 100 μm of the tumor boundary exhibit white tracks. Image is representative of the average macrophage response to 6 separate collagen tumors. (E) Track displacement and total track length was quantitated for macrophage migration within and beyond 100 μm of the collagen tumor boundary (mean ± SEM; *n* = 15 macrophages within 100 μm and 15 macrophages beyond 100 μm of the collagen tumor boundary). # denotes a significant difference in migration path displacement ($p < 0.05$). ## denotes a significant difference in total migration path length ($p < 0.0001$).

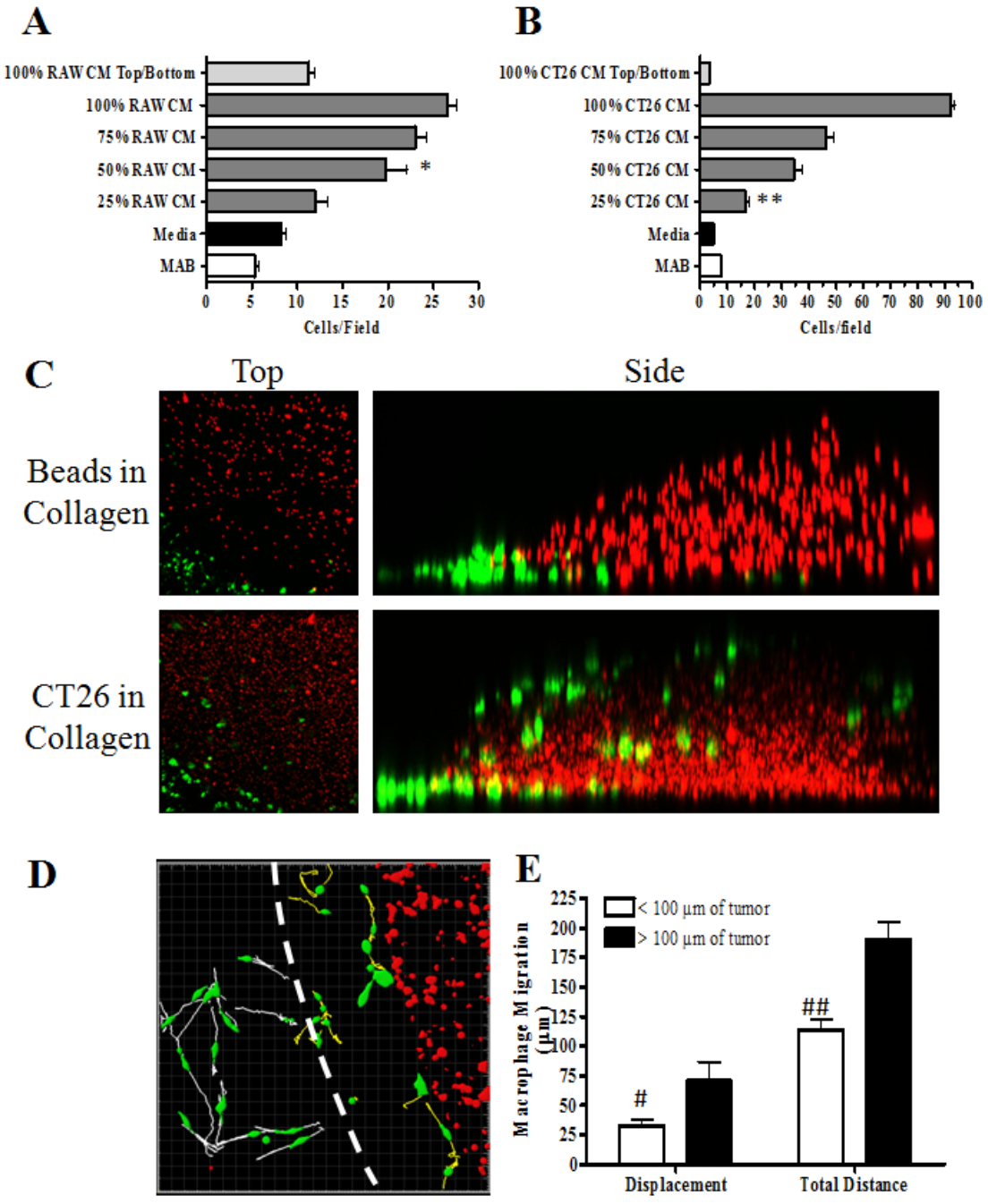
A
100% RAW CM Top/Bottom
100% RAW CM
75% RAW CM
50% RAW CM
25% RAW CM
Media
MAB
*
0 5 10 15 20 25 30
Cells/Field
B
100% CT26 CM Top/Bottom
100% CT26 CM
75% CT26 CM
50% CT26 CM
25% CT26 CM
Media
MAB
**
0 10 20 30 40 50 60 70 80 90 100
Cells/field
C
Top
Side
Beads in Collagen
CT26 in Collagen
D
E
< 100 µm of tumor
> 100 µm of tumor
Macrophage Migration (µm)
225 200 175 150 125 100 75 50 25 0
#
##
Displacement
Total Distance

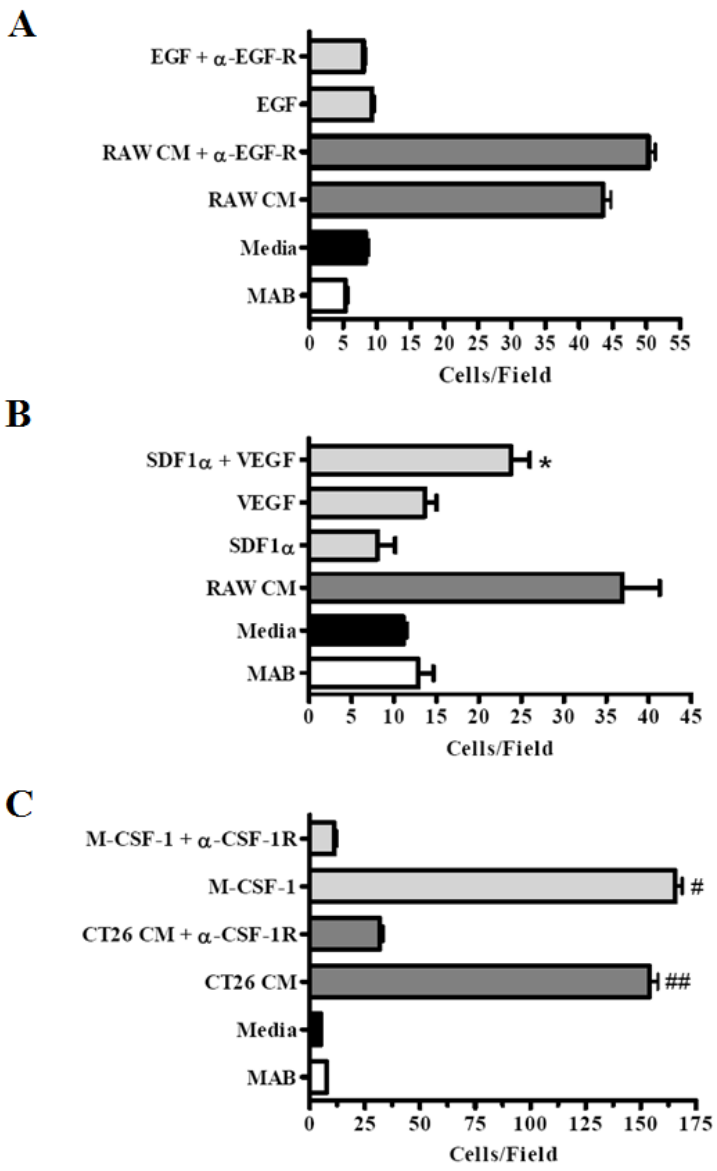

Figure 4. CSF-1, VEGF and SDF-1α mediate co-chemotaxis between RAW 264.7 macrophages and CT26 tumor cells. (A) CT26 were added to the upper well of a Boyden chamber with RAW 264.7 conditioned media, 100 ng/ml EGF in migration buffer, control migration buffer or complete DMEM added to the lower well. Anti-EGFR was present in both the top and bottom wells, as indicated, throughout the experiment. (B) CT26 were added to the upper well of a Boyden chamber with 100 ng/ml SDF-1α, 10 ng/ml VEGF, SDF-1α + VEGF, RAW 264.7 conditioned media, control migration buffer or complete DMEM added to the lower well. * denotes significance between SDF-1α with VEGF compared to SDF-1α ($p < 0.05$) or VEGF alone ($p < 0.05$). (C) RAW 264.7 were added to the upper well of a Boyden chamber with 40 ng/ml CSF-1, CT26 conditioned media, control buffer or complete DMEM added to the lower well. Anti-CSF-1R was present in both top and bottom wells, as indicated, throughout the assay. # denotes significance between CSF-1 and CSF-1 + anti-CSF-1R ($p < 0.0001$). ## denotes significance between CT26 CM and CT26 CM + anti-CSF-1R ($p < 0.0001$). (mean ± SEM; n = 15-30 randomly selected fields over 3-6 separate experiments for all data).

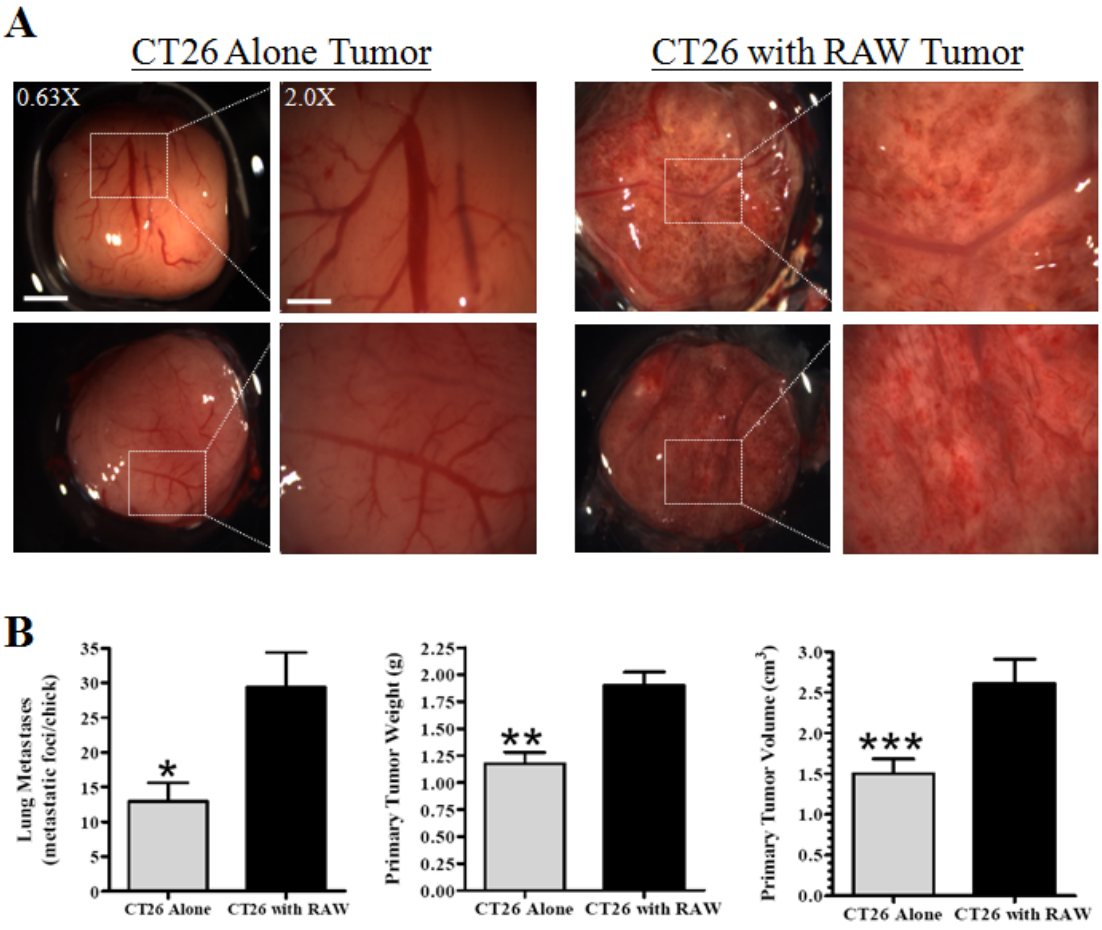

Figure 5. RAW macrophages promote CT26 tumor formation, metastasis and neovascularization in the chick CAM. A) CT26-DsRed alone or with RAW-GFP were inoculated onto CAMs at 9 d. Tumors were developed for 11 d. (A) Tumors were imaged by stereomicroscope (0.63X, scale bar: 3.5 mm; *inset* 2.0X, scale bar: 1 mm). Images are representative of tumors from 3-4 separate experiments. B) Chick embryos were harvested at 20 d. The number of GFP expressing cells/cell clusters in the lungs was determined by fluorescent microscopy (mean ± SEM; n = 14-16 lungs over 3-4 experiments). * denotes significance between primary tumors with CT26 alone compared to primary tumors with CT26 and RAW 264.7 ($p < 0.01$). Explanted tumors were also analyzed for weight and volume. (mean ± SEM; n = 10-11 tumors over 2-3 separate experiments). ** denotes significance in weight between primary tumors with CT26 alone compared to primary tumors with CT26 and RAW 264.7 ($p < 0.001$). *** denotes significance in volume between primary tumors with CT26 alone compared to primary tumors with CT26 and RAW 264.7 ($p < 0.001$).

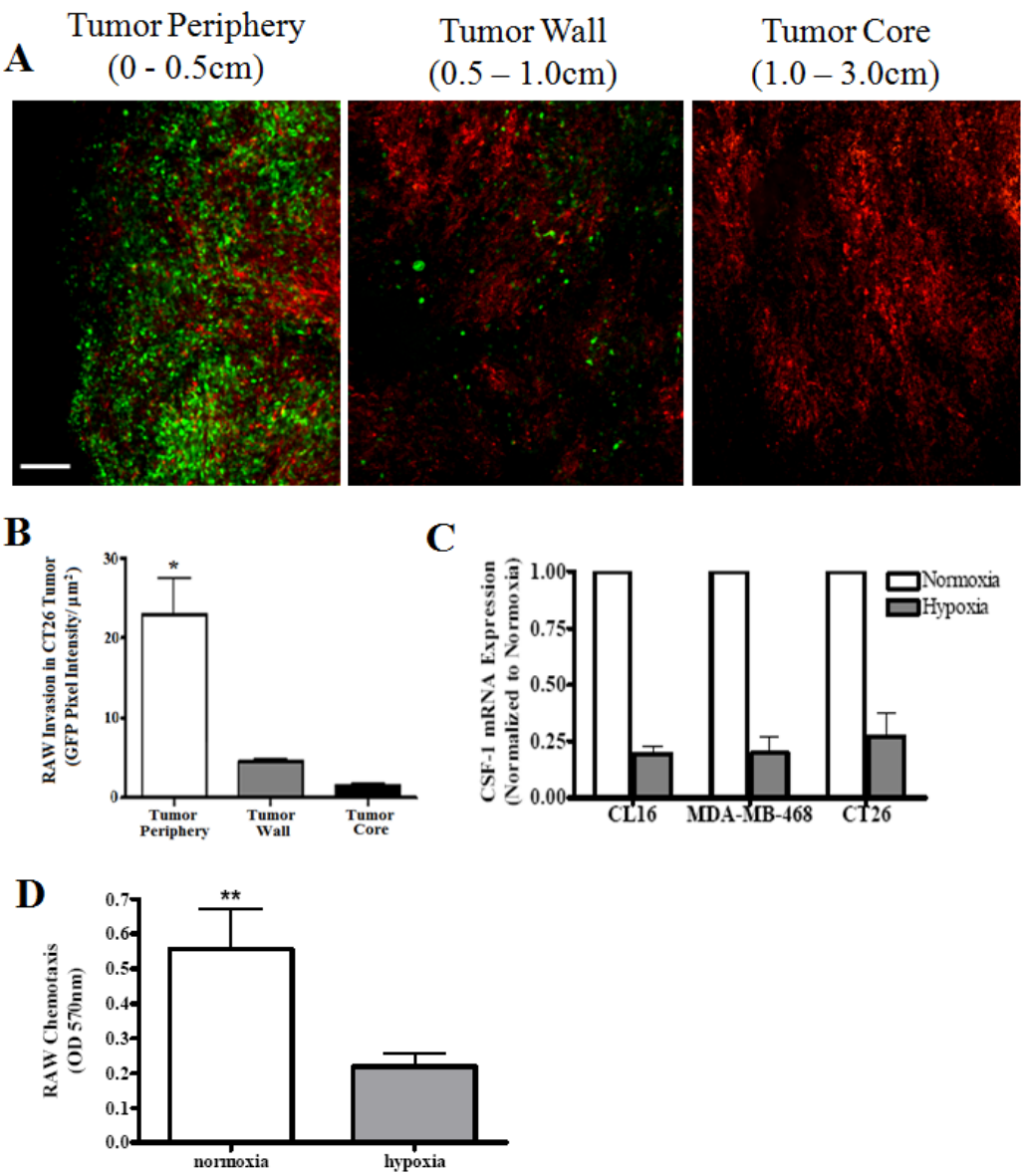

Figure 6. Analysis of macrophage localization in CT26 tumors *in vivo*. (A) Tumors were imaged at 0 cm from the periphery (Tumor Periphery), 0.5 cm from the periphery (Tumor Wall) and 1.0 cm from the tumor periphery (Tumor Core). Images are representative of tumors from 3-4 separate experiments. (B) RAW-GFP distribution within the mixed cell tumors was determined by averaging pixel bit maps to produce a mean fluorescence intensity for each region of the tumor. Data represents the average ± SEM for RAW-GFP distribution in tumors from 3 separate experiments. * denotes significance in pixel intensity between the tumor periphery region and the tumor wall region ($p < 0.001$). (C) CSF-1 mRNA expression under hypoxic conditions is presented as a percentage of basal expression under normoxic conditions. HPRT-1 was used to normalize by global gene expression. Data represents the average ± SEM from 3 separate experiments. (D) RAW 264.7 were added to the upper well of a Boyden chamber with complete DMEM added to the lower well. RAW 264.7 were allowed to migrate for 24 hrs at 37°C under normoxic (21% oxygen) or hypoxic (1% oxygen) (mean ± SEM; n = 15-30 randomly selected fields over 3 separate experiments). ** denotes significance between RAW chemotaxis during hypoxic and normoxic conditions ($p < 0.05$).

Table 1. Microarray analysis of inflammatory gene expression during co-culture of tumor cells and macrophages. CT26 cells were incubated in RAW 264.7 CB, and vice versa, for 24hrs prior to mRNA isolation and analysis using the Codelink Mammalian Inflammation Bioarray. Significance of transcript upregulation or downregulation was determined using the VAMPIRE statistical algorithm. Data represents the fold change in transcript expression from 3 separate experiments. Of the 270 genes detected in RAW 264.7 (right) and the 85 genes detected in CT26 (left), the most highly upregulated or downregulated genes associated with migration, proliferation and angiogenesis are presented.

CT26 Colon Cancer Cells in RAW CB			RAW Macrophages in CT26 CB		
Gene	Description	CB/Ctrl	Gene	Description	CB/Ctrl
FGF10	Fibroblast Growth Factor 10	0.3	uPA	Urokinase Plasminogen Activator	0.3
CD80	CD80Antigen	0.6	LTB	Lymphotoxin B	0.6
HSP1A	Heat Shock Protein 1A	0.6	CCL4	Chemokine (C-C motif) Ligand 4	0.6
SOCS1	Suppressor of Cytokine Signaling 1	0.7	IL8Rα	Interleukin 8 Receptor, Alpha	0.6
CD14	CD14 Antigen	0.0	MMP2	Matrix Metallopeptidase 2	0.6
VEGF-A	Vascular Endothelial Growth Factor A	1.5	TNF-α	Tumor Necrosis Factor alpha	0.8
RelA	V-rel Reticuloendotheliosis Viral Oncogene Homolog A	1.5	CCR1	Chemokine (C-C motif) Receptor 1	1.2
TGFβ3	Transforming Growth Factor, Beta 3	1.6	IL18	Interleukin 18	1.2
CXCL10	Chemokine (C-X-C motif) Ligand 10	1.6	Vim	Vimentin	1.2
TGFβ1	Transforming Growth Factor, Beta 1	1.8	RelA	V-rel Reticuloendotheliosis Viral Oncogene Homolog A	1.2
ARHGEF2	Rho/Rac Guanine Nucleotide Exchange Factor 2	1.8	CtsD	Cathepsin D	1.3
RalGDS	Ral Guanine Nucleotide Dissociation Stimulator	1.9	TGFβ1	Transforming Growth Factor, Beta 1	1.3
NF_kB1_b	NFκB Inhibitor Beta	1.9	Casp8	Caspase 8	1.3
Arrb2	Beta 2 Arrestin	2.0	Arrβ2	Beta 2 Arrestin	1.3
NF_kB2	NFkB 2	2.1	Vav1	Vav 1 Oncogene	1.3
IL15Ra	Interleukin 15 Receptor, Alpha Chain	2.2	IL16	Interleukin 16	1.4
RelB	Avian Reticuloendotheliosis Viral Oncogene Related B	2.4	ILK	Integrin Linked Kinase	1.4
CSF1	Colony Stimulating Factor 1	2.6	XCR1	Chemokine (C motif) Receptor 1	1.4
NF_kB1_a	NFkB Inhibitor Alpha	2.7	IL11Rα1	Interleukin 11 Receptor, Alpha Chain 1	1.4
VCAM1	Vascular Cell Adhesion Molecule 1	3.0	ITGβ2	Beta 2 Integrin	1.5
CXCL1	Chemokine (C-X-C motif) Ligand 1	3.1	CXCL2	Chemokine (C-X-C motif) Ligand 2	1.6
CCL2	Chemokine (C-C motif) Ligand 2	3.2	CSF2Rβ2	Colony Stimulating Factor 2 Receptor, Beta 2	1.6
MMP10	Matrix Metallopeptidase 10	3.3	IL1R-L1	Interleukin 1 Receptor-like 1	1.7
CCL20	Chemokine (C-C motif) Ligand 20	3.8	IL15Rα	Interleukin 15 Receptor, Alpha Chain	1.7
NF_kB1_s	NFkB Inhibitor Epsilon	4.8	NCAM1	Neural Cell Adhesion Molecule-1	1.8
CSF2	Colony Stimulating Factor 2	5.1	VEGF-A	Vascular Endothelial Growth Factor A	1.8
CXCL2	Chemokine (C-X-C motif) Ligand 2	6.7	CD14	CD14 Antigen	1.9
INFα9	Interferon Alpha 9	9.3	CXCL12	Chemokine (C-X-C motif) Ligand 12	2.3

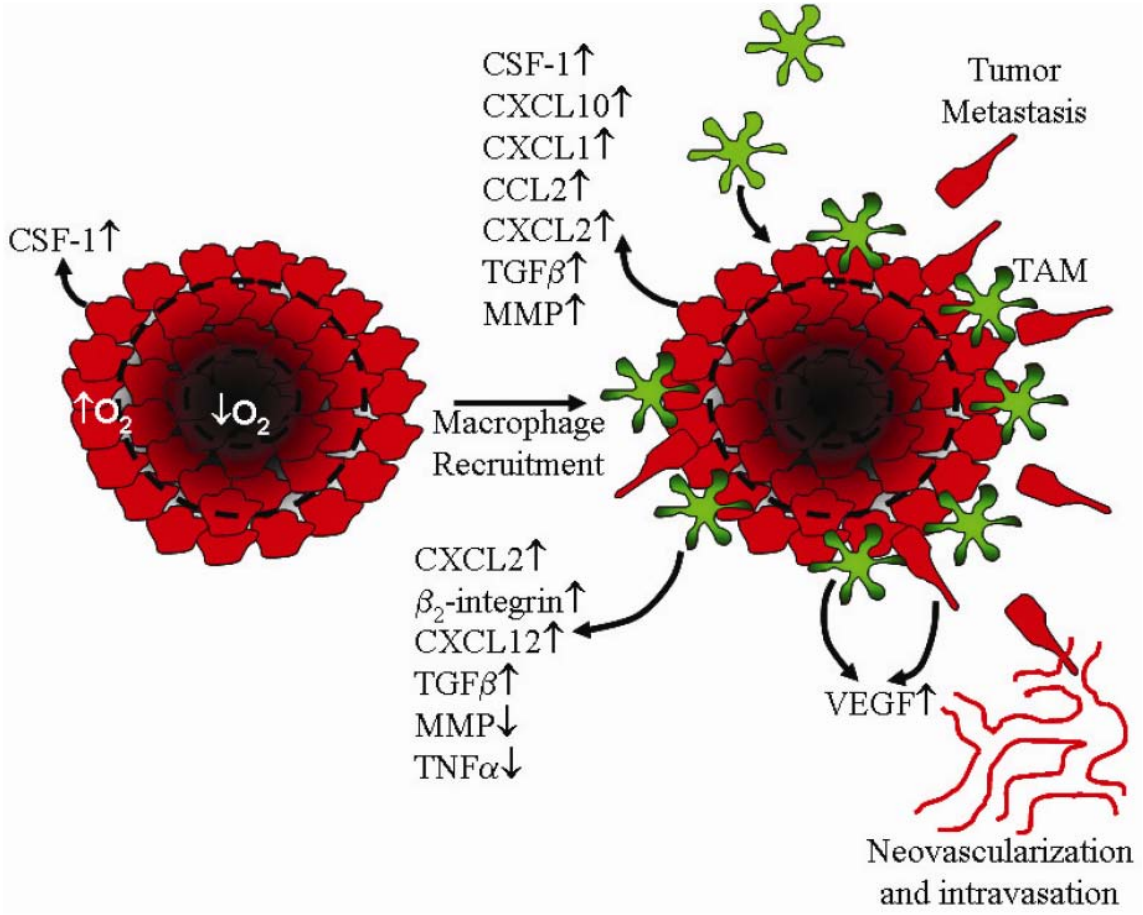

Figure 7. Proposed model for the role of tumor associated macrophages in cancer progression. During tumor growth, macrophages home to normoxic regions at the tumor periphery in response to secreted CSF-1. The macrophages in turn release soluble chemokines that stimulate the tumor cells to release more CSF-1 creating a localized high concentration of CSF-1 that promotes further macrophage infiltration and survival at the tumor periphery. The close proximity of macrophages and tumor cells establishes a paracrine chemokine network at the tumor margin that results is at least two major outcomes. First, tumor cell migration and tissue invasion increases as the result of SDF-1α and VEGF release by tumor associated macrophages. Second, both tumor cells and macrophages are stimulated to release VEGF and TGFβ, which facilitates vessel growth, remodeling, and increased permeability. The increase in tumor cell invasiveness combined with structural changes in the surrounding vasculature provides optimal conditions for tumor cell intravasation and metastasis

Green etal.
Supplemental Figure S1

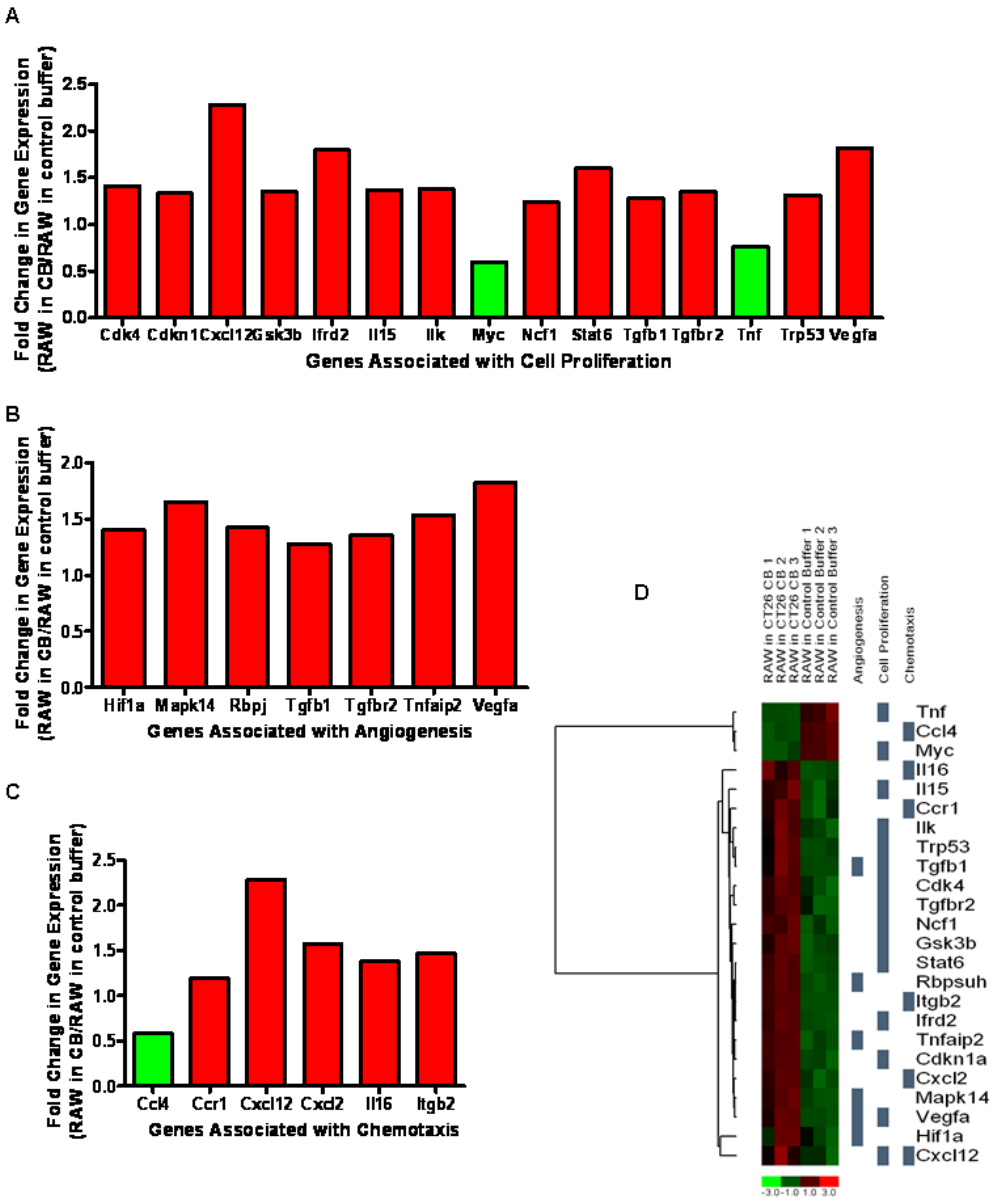

Figure S1. Hierarchical clustering of gene transcripts upregulated and downregulated by RAW 264.7 macrophages in CT26 conditioned buffer. Of the 854 inflammatory genes examined, 270 were differentially expressed. Hierarchical clustering of this subpopulation was performed using dChip (distance: correlation, linkage: centroid) based on the gene ontology annotations for A) cell proliferation, B) angiogenesis and C) chemotaxis. Red bars and green bars denote upregulated and downregulated genes, respectively. D) For heatmap analysis, intensity scores were calculated based on the significance of gene up- or down-regulation, as determined by VAMPIRE analysis. These genes were then organized based on the gene ontology annotations for angiogensis, cell proliferation and chemotaxis using dChip (distance metric: correlation, linkage method: average). Each column in the heatmap represents an independent replicate of RAW 264.7 in CT26 conditioned buffer or RAW 264.7 in standard control buffer, as indicated.

Green etal.
Supplemental Figure S2

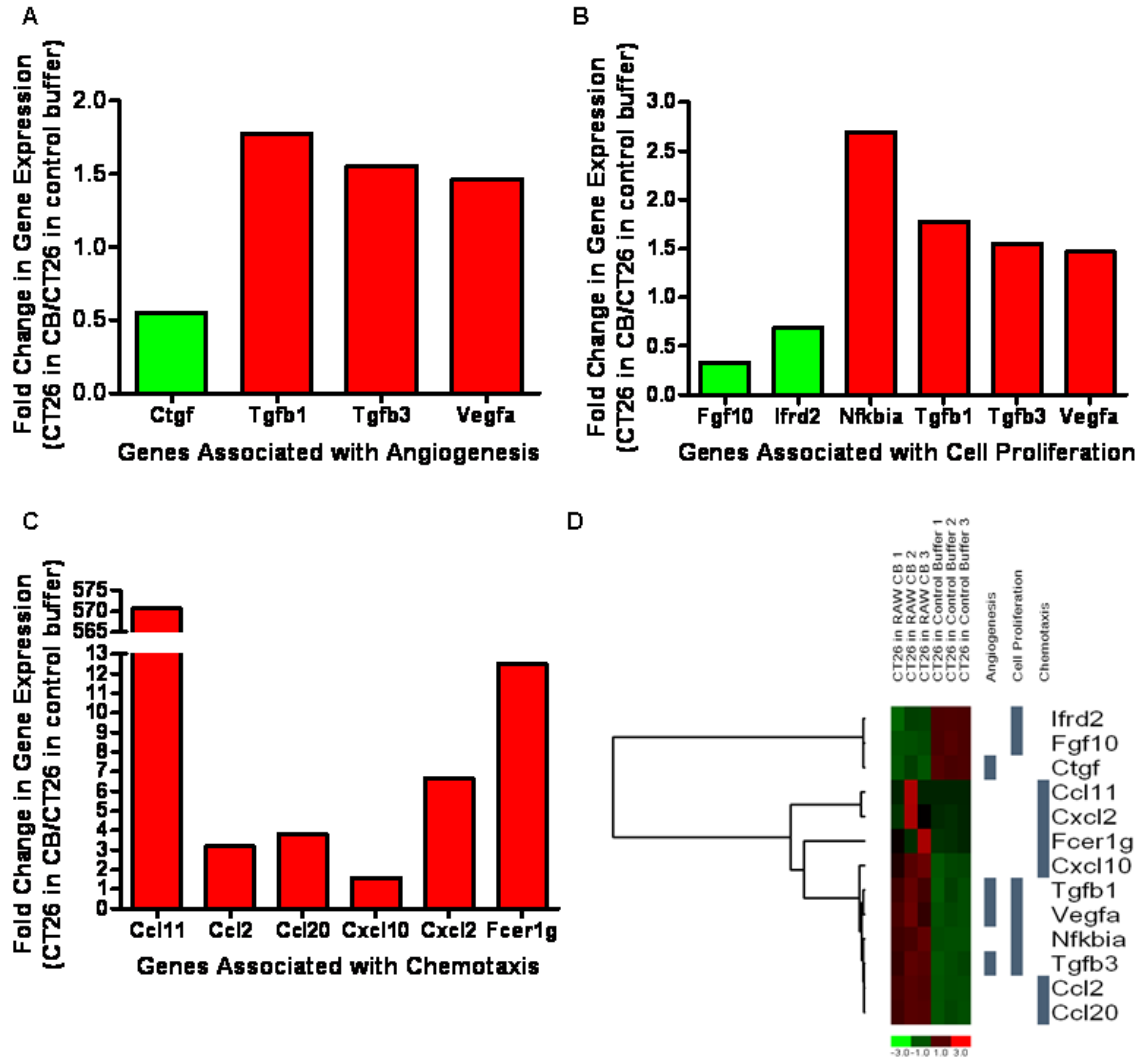

Figure S2. Hierarchical clustering of gene transcripts upregulated and downregulated by CT26 tumor cells in RAW 264.7 conditioned buffer. Of the 854 inflammatory genes examined, 85 were differentially expressed. Hierarchical clustering of this subpopulation was performed using dChip (distance: correlation, linkage: centroid) based on the gene ontology annotations for A) angiogensis, B) cell proliferation and C) chemotaxis. Red bars and green bars denote upregulated and downregulated genes, respectively. D) For heatmap analysis, intensity scores were calculated based on the significance of gene up- or down-regulation, as determined by VAMPIRE analysis. These genes were then organized based on the gene ontology annotations for angiogensis, cell proliferation and chemotaxis using dChip (distance metric: correlation, linkage method: average). Each column in the heatmap represents an independent replicate of CT26 tumor cells in RAW 264.7 conditioned buffer or CT26 in standard control buffer, as indicated.

References

1. Tlsty TD, Coussens LM (2006) Tumor stroma and regulation of cancer development. *Annu Rev Pathol* 1: 119-150.

2. Lewis CE, Leek R., Harris A, McGee JO (1995) Cytokine regulation of angiogenesis in breast cancer: the role of tumor-associated macrophages. *J. Leukoc. Biol*. 57: 747–751.

3. Pollard JW (2004) Tumour-educated macrophages promote tumour progression and metastasis. *Nat Rev Cancer*. 4:71-78.

4. Chitu V, Stanley ER (2006) Colony-stimulating factor-1 in immunity and inflammation. *Current Opinion Immunol* 18:39-48.

5. Condeelis J, Segall JE (2003). Intravital Imaging of Cell Movement in Tumors. *Nature Rev. Cancer* 3: 921-930

6. Yamashiro S, Takeya M, Nishi J, Kuratsu T, Yoshimura Y, Ushio Y, Takahashi K. (1994) Tumor derived monocyte chemoattractant protein-1 induces intratumoral infiltration of monocyte-derived macrophage subpopulation in transplanted rat tumors. *Am J Pathol* 145: 856–867.

7. Sica A, Allavena P, Mantovani A (2008) Cancer related inflammation: the macrophage connection. *Cancer Lett* 267: 204–215.

8. Mantovani A, Sozzani S, Locati M, Allavena P, Sica A (2002) Macrophage polarization: tumor-associated macrophages as a paradigm for polarized M2 mononuclear phagocytes. *Trends Immunol* 23: 549–555.

9. Lewis CE, Pollard JW. (2006) Distinct role of macrophages in different tumor microenvironments. *Cancer Res* 66: 605–12.

10. Ohno S, Ohno Y, Suzuki N, Kamei T, Koike K, Inagawa H, Kohchi C, Soma GI, Inoue M (2004) Correlation of histological localization of tumor-associated macrophages with clinicopathological features in endometrial cancer. *Anticancer Res* 24: 3335–3342.

11. O'Sullivan C, Lewis CE, Harris AL, McGee JO (1993) Secretion of epidermal growth factor by macrophages associated with breast carcinoma. *Lancet* 342: 148–149.

12. Pusztai L, Clover LM, Cooper K, Starkey PM, Lewis CE, McGee JO (1994) Expression of tumour necrosis factor alpha and its receptors in carcinoma of the breast. *Br J Cancer* 70: 289–292.

13. Leek RD, Harris AL (2002) Tumor-associated macrophages in breast cancer. *J Mammary Gland Biol Neoplasia* 7: 177–189.

14. Leek RD, Harris AL, Lewis CE. (1994) Cytokine networks in solid human tumors: regulation of angiogenesis. *J. Leukoc. Biol.* 56:423-435.

15. Stoletov K, Montel V, Lester RD, Gonias SL, Klemke R. (2007) High-resolution imaging of the dynamic tumor cell-vascular interface n transparent zebrafish. *PNAS.* 104: 17406-17411.

16. Leek RD, Lewis CE, Whitehouse R, Greenall M, Clarke J, Harris AL. (1996) Association of macrophage infiltration with angiogenesis and prognosis in invasive breast carcinoma. *Cancer Res* 56, 4625– 4629.

17. Grimshaw MJ, Balkwill FR. (2001) Inhibition of monocyte and macrophage chemotaxis by hypoxia and inflammation – a potential mechanism. *Eur J Immunol* 31: 480–489.

18. Crowther M, Brown NJ, Bishop ET, Lewis CE. (2001) Microenvironmental influence on macrophage regulation of angiogenesis in wounds and malignant tumors. *J Leukoc Biol* 70:478–90.

19. Murdoch C, Giannoudis A, Lewis CE. (2004) Mechanisms regulating the recruitment of macrophages into hypoxic areas of tumors and other ischemic tissues. *Blood*. 104:2224-2234.

20. Burke B, Tang N, Corke KP, Tazzyman D, Ameri K, Wells M, Lewis CE (2002) Expression of HIF-1alpha by human macrophages: implications for the use of macrophages in hypoxia-regulated cancer gene therapy. *J Pathol* 196: 204–212

21. Talks KL, Turley H, Gatter KC, Maxwell PH, Pugh CW, Ratcliffe PJ, Harris AL (2000) The expression and distribution of the hypoxia-inducible factors HIF-1alpha and HIF-2alpha in normal human tissues, cancers, and tumor-associated macrophages. *Am J Pathol* 157: 411–421.

22. Mantovani A, Allavena P, Sozzani S, Vecchi A, Locati M, Sica A (2003). Chemokines in the recruitment and shaping of the leukocyte infiltrate of tumors. *Sem. In Cancer Biol.* 14: 155-160.

23. Condeelis J, Pollard JW. (2006) Macrophages: obligate partners for tumor cell migration, invasion and metastasis. *Cell*. 124: 263-266.

24. Locati M, Deuschle U, Massardi ML, Martinez FO, Sironi M, Sozzani S, Bartfai T, Mantovani A (2002) Analysis of the gene expression profile activated by the CC

chemokine ligand 5/RANTES and by lipopolysaccharide in human monocytes. *J Immunol*, 168: 3557–3562.

25. Wyckoff J, Wang W, Lin EY, Wang Y, Pixley F, Stanley ER, Graf T, Pollard JW, Segall J, Condeelis J (2004) A paracrine loop between tumor cells and macrophages is required for tumor cell migration in mammary tumors. *Cancer Res* 64: 7022–7029.
26. Lin EY, Nguyen AV, Russell RG, Pollard JW. (2001) Colony-stimulating factor 1 promotes progression of mammary tumors to malignancy. *J Exp Med*. 193: 727-739.

27. Muller A, Homey B, Soto H, Ge N, Catron D, Buchanan ME, McClanahan T, Murphy E, Yuan W, Wagner SN, Barrera JL, Mohar A, Verastegui E, Zlotnik A (2001) Involvement of chemokine receptors in breast cancer metastasis. *Nature* 410:50-56.

28. Bingle L, Brown NJ and Lewis CE. (2002) The role of tumour associated macrophages in tumour progression: implications for new anticancer therapies. *J Pathol* 196: 254-265.

29. Nakayama Y, Nagashima N, Minagawa N, Inoue Y, Katsuki T, Onitsuka K, Sako T, Hirata K, Nagata N, Itoh H. (2002) Relationships between tumor associated macrophages and clinicopathological factors in patients with colorectal cancer. *Anticancer Res.* 22:4291-4296.

30. Montel V, Huang TY, Mose E, Pestonjamasp K, Tarin D. (2005) Expression profiling of primary tumors and matched lymphatic and lung metastases in a xenogeneic breast cancer model. *Am J Path.* 166:1565-1579.

31. Klemke RL, Shuang C, Giannini AL, Gallagher PJ, de Lanerolle P, Cheresh DA. (1997) Regulation of cell motility by mitogen-activated protein kinase. *J. Cell Biol.* 137: 481-492.

32. Cho SY, Klemke RL. (2000) Extracellular-regulated kinase activation and CAS/Crk coupling regulate cell migration and suppress apoptosis during invasion of the extracellular matrix. *J. Cell. Biol.* 149:223-236.

33. Hsiao A, Worrall DS, Olefsky JM, Subramaniam S. (2004) Variance-modeled posterior inference of microarray data: detecting gene-expression changes in 3T3-L1 adipocytes. *Bioinformatics*. 20: 3108-3127.

34. Lester RD, Jo M, Montel V, Takimoto S, Gonias SL. (2007) uPAR induces epithelial-mesenchymal transition in hypoxic breast cancer cells. *J. Cell Biol.* 178: 425-436.

35. Klemke RL, Leng J, Molander R, Brooks PC, Vuori K, Cheresh DA. (1998) CAS/Crk coupling serves as a "molecular switch" for induction of cell migration. *J. Cell Biol.* 140: 961-972.

36. Friedl P, Wolf K. (2003) Tumour-cell invasion and migration: diversity and escape mechanisms. *Nature Rev Cancer.* 3:362-374.

37. Mantovani A, Sica A, Sozzani S, Allavena P, Vecchi A, Locati M. (2004) The chemokine system in diverse forms of macrophage activation and polarization. *Trends in Immunol*. 25: 677-686.

38. Hagemann T, Wilson J, Burke F, Kulbe H, Fiona N, Pluddemann A, Charles K, Gordon S, Balkwill FR. (2006) Ovarian cancer cells polarize macrophages toward a tumor-associated phenotype. *J Immunol*. 176: 5023-5032.

39. Kluger HM, Lev DC, Kluger Y, McCarthy MM, Kiriakova G, Camp RL, Rimm DL, Price JE. (2005) Using a xenograft model of human breast cancer metastasis to find genes associated with clinically aggressive disease. *Cancer Res*. 65: 5578-5587.

40. Minn AJ, Gupta GP, Siegel PM, Bos PD, Shu W, Giri DD, Viale A, Olshen AB, Gerald WL, Massgue J. (2005) Genes that mediate breast cancer metastasis to lung. *Nature* 436: 518-524.

41. Weis S, Cui JH, Barnes L, Cheresh D. (2004) Endothelial barrier disruption by VEGF-mediated src activity potentiates tumor cell extravasation and metastasis. *J Cell Biol*. 167:223-229.

42. Bierie B, Moses HL. (2006) TGFβ: the molecular Jekyll and Hyde of cancer. *Nat Rev Cancer*. 6:506-520.

43. Goswami S, Sahai E, Wyckoff JB, Cammer M, Cox D, Pixley FJ, Standley R, Segall JE, Condeelis JS. (2005) Macrophages promote the invasion of breast carcinoma cells via a colony-stimulating fctor-1/epidermal growth factor paracrine loop. *Cancer Res*. 65: 5278-5283.

44. Lin EY, Li JF, Bricard G, Wang WG, Deng Y, Sellers R, Porcelli SA, Pollard JW. (2007) Vascular endothelial growth factor restores delayed tumor progression in tumors depleted of macrophages. *Mol Oncol.* 1: 288-302.

45. Kryczek I, Wei S, Keller E, Liu R, Zou W (2007) Stroma-derived factor (SDF-1/ CXCL12) and human tumor pathogenesis. *Am J Physiol Cell Physiol* 292: C987–995.

46. Kim J, Yu W, Kovlasi K, Ossowski L. (1998) Requirement for specific proteases in cancer cell intravasation as revealed by a novel semiquantitative PCR-based assay. *Cell*. 94:353-362.

47. Sutton A, Friand V, Brule-Donneger S, Chaigneau , Ziol M, Sainte-Catherine O, Poire A, Saffar L, Kraemer M, Vassy J, Nahon P, Salzmann JL, Gattegno L,

Chamaux N. (2007) Stromal cell-derived factor1/chemokine (C-X-C motif) ligand 12 stimulates human hepatoma cell growth, migration and invasion. *Mol Cancer Res.*5: 21-33.

48. Gupta SK, Lysko PG, Pillarisett K, Ohlstein E, Stadel JM (1998) Chemokine receptors in human endothelial cells. Functional expression of CXCR4 and its transcriptional regulation by inflammatory cytokines. *J. Biol. Chem.* 273: 4282–4287.

49. Salcedo, R. Wasserman K, Young HA, Grimm MC, Howard OMZ, Anver MR, Kleinman HK, Murphy WJ, Oppenheim JJ (1999) Vascular endothelial growth factor and basic fibroblast growth factor induce expression of CXCR4 on human endothelial cells: *in vivo* neovascularization induced by stromal-derived factor-1α. *Am. J. Pathol.* 154: 1125–1135.

50. Homey B, Muller A, Zlotnik A (2002) Chemokines: Agents for the Immunotherapy of Cancer? *Nature Rev. Immunol* 2:175-184.

51. Dougherty ST, Eaves CJ, McBride WH, Dougherty GJ (1997) Role of macrophage-colony-stimulating factor in regulating the accumulation and phenotype of tumor-associated macrophages. *Cancer Immunol Immunother* 44:165-172.

52. Lewis JS, Landers RJ, Underwood JC, Harris AL, Lewis CE (2000) Expression of vascular endothelial growth factor by macrophages is up-regulated in poorly vascularized areas of breast carcinomas. *J Pathol* 192: 150–158.

53. Hagemann T, Robinson SC, Schulz M, Trumper L, Balkwill FR, Binder C. (2004) Enhanced invasiveness of breast cancer cell lines upon co-cultivation with macrophages is due to a TNF-α dependent up-regulation of matrix metalloproteases. *Carcinogenesis*. 25:1543-1549.

54. Hauptmann S, Zwadlo-Klarwasser G, Jansen M, Klosterhalfen B, Kirkpatrick CJ (1993) Macrophages and Multicellular Tumor Spheroids in Co-Culture: A Three-Dimensional Model to Study Tumor-Host Interactions: Evidence for Macrophage-Mediated Tumor Cell Proliferation and Migration. *Am J. Pathol.*143:1406-1415.

.